ASSESSMENT OF THE BENTHIC IMPACTS OF RAISED GROUNDGEAR FOR THE EASTERN BERING SEA POLLOCK FISHERY

A Thesis

Presented to the Faculty of

Alaska Pacific University

In Partial Fulfillment of the Requirements

For the Degree of

Master of Science in Environmental Science

By

Susan L. Zagorski

December 2016

ACKNOWLEDGEMENTS

I would first and foremost like to thank my advisor Dr. Brad Harris for all of his support since his arrival at Alaska Pacific University. I had always known I had a passion for fisheries, then Dr. Brad Harris introduced me to the world of conservation engineering and fishery science, and my passion has grown. I appreciate his enthusiasm and encouragement to become involved in the Alaska fisheries. Dr. Harris has inspired me to be the greatest version of myself, stay enthusiastic and to not let anything get in my way. Dr. Craig Rose has also been such a meaningful mentor. The passion he has for fisheries and his brilliance truly inspires me. I appreciate him for all he has taught me and for all the support he has provided, especially in the field and in Seattle. Committee member Dr. Pingguo He, despite being on opposite coasts, has taught me so much about fishery science and gear design. Whether it was through his writing or at conferences and workshops he was always there to encourage me and help me go further in the field of conservation engineering. Ed Richardson and the entire crew at the At-Sea Processors Association have been amazing mentors; I look up to all of them. I appreciate that Ed has always challenged me to look further and think harder. I really appreciate the crew of the F/V Great Pacific, they have been nothing but supportive and have done so much for this project. Lastly, I have to thank the entire Fisheries, Aquatic Science and Technology Lab; those who directly helped with this project and those who have just been there to share fish stories with. I will never forget the endless hours spent in the lab.

ABSTRACT

The Alaska pollock *(Gadus chalcogrammus)* fishery in the Eastern Bering Sea (EBS) is a major contributor to domestic and global fish production. However, regulations governing groundgear construction (trawl components that contact the seafloor) have limited opportunities to experiment with new gear designs aimed at minimizing potential effects on the seafloor and Essential Fish Habitat (EFH). In this thesis, alternative trawl footropes designed to fish just above the seafloor were tested. The designs varied by weight and rope materials, and were evaluated based on reduced seafloor contact, impacts to structure forming invertebrates, and effective height above the seafloor. Video and sonar data were used to compare seafloor contact and sea whip (*Halipteris willemoesi*) condition between impacted areas and adjacent unaffected control areas. The designs successfully reduced direct seafloor contact by 95-97% of the nominal contact. A susceptibility analysis showed 2.4 - 16.1% more downed sea whips in impacted areas than in control areas. The contact and susceptibility impacts were greater with footropes comprised of heavy rope materials than more buoyant materials.

Bottom contact sensors were used to determine the height of the footrope above the seafloor, and 117 mean measurements of height above the seafloor were obtained. For the footrope components, 75% were raised more than 10.2 cm (4 in) above the seafloor, enough height to avoid most benthic features. While work is still required to determine the implications of these modifications for target species catch and bycatch, these results indicate a potential for substantial reductions of benthic interactions with trawl gear.

TABLE OF CONTENTS

LIST OF TABLES

LIST OF FIGURES

GENERAL INTRODUCTION

All of the commercial fishery species harvested globally either live on or near the seabed or employ life history strategies that are linked to benthic processes (NMFS 2016, FAO 2016). The act of pursuing and catching benthic and demersal species requires operating fishing gear on or very near the seabed, often resulting in direct gear-seabed contact. Generally, the extent and distribution of benthic habitats and the locations and impacts of fishing disturbances are poorly understood (Kaiser et al. 2016). Globally about 20% of wild fish and shellfish are caught with bottom tending fishing gear. It is important to measure the effect that gear has on benthic features and the seafloor (Watson et al. 2006, Kaiser et al. 2016). In the USA, the Magnuson Stevens Fisheries Conservation and Management Act requires fishery management plans to identify, describe, and conserve Essential Fish Habitat (EFH); EFH is defined as "*those waters or substrates that are necessary to fish for spawning, breeding, feeding, and growth to maturity*" (16 U.S.C. § 3(10)). Regional Fisheries Management Councils are then required to minimize the adverse impacts of fishing on EFH (50 CFR § 600.815).

The Bering Sea Aleutian Islands (BSAI) Alaska pollock fishery catches about 30% of the fish (by weight) landed in USA water (APA 2016). The permissible gear in this fishery must comply with pelagic trawl construction regulations (He and Winger 2010). These regulations require the trawl to have a bare chain footrope and no lifting or protective elements attached to the head- or footrope (50 CFR § 679.24). Given the low vertical distribution of pollock in the water column (Honkalehto et al. 2008, Tsuji 1989), variable contact with the seafloor during fishing can be assumed while targeting pollock with this gear. The National Marine Fisheries Service (NMFS) manual on acoustic assessment methodology of pollock notes the difficulty of discriminating adult pollock signals from the seabed (NMFS 2004).

The interactions between fishing gear and the seabed can produce adverse impacts (Thrush and Dayton 2002). The impacts depend on gear type, substrate type, features present, and the area's natural disturbance (He and Winger 2010). Conserving benthic habitats may be accomplished by means of area closures, limits on fishing and gear modifications (NRC 2002). Of these, gear modifications (e.g. raising trawl footropes) show potential, but empirical evaluations of their effects are scarce.

Raising the clump weights and footrope (also referred to as groundgear throughout this thesis) off the seabed may reduce the interactions between fishing gear and benthic features. These types of modifications are sensible given that the actual distributions of benthic features, their interaction rates with fishing gear, and their rates of recovery are poorly understood (Kaiser et al. 2016, Nimick and Harris in Press, Grabowski et al. 2014). Raised groundgear modifications are primarily designed for bottom trawls which contact the seafloor. Guyonnet et al. in 2008 modified the bridles of a bottom (otter) trawl with lighter material (14mm Dyneema® cable with 4mm chain) to produce less seafloor contact during fishing. Before and after impacts to macro- and megafauna were compared via an impact and control sampling design which showed that measured impacts to macro- and megafauna from the modified bridles had no significant difference between control and impact sites. However, in the impacted sites of the tested conventional trawl significant impacts to macrofauna were observed. Similarly, Rose et al. (2010 a&b) modified sweeps of a bottom trawl by adding small, widely-spaced disks to the sweeps so that the cables were slightly lifted (5, 7.5, and 10 cm) off the seafloor. The gear was towed parallel to a bottom trawl with conventional sweeps. The impacts of the modified sweeps were evaluated by measuring the scars in the seafloor created by direct seafloor contact and comparing the impact to that of the conventional sweeps. The modified sweeps showed 95% less contact area compared to the conventional sweeps (Rose et al. 2010 a&b). Shortly thereafter, the raised-sweep gear modifications were accepted by fishery managers and the gear regulations for the BSAI flatfish fishery were amended (NPFMC 2010).

In order for a raised footrope modification to be considered effective for conserving EFH, it must minimize adverse impacts, defined as: “*those that are more than minimal and not temporary in nature”* (NPFMC 2016). In this thesis, raised footrope modifications with various light-weight materials and bobbins were constructed, attached to a conventionally constructed pelagic trawl, and their direct seafloor contact evaluated by trawling on the seafloor. To evaluate whether the footrope modifications reduced impacts to benthic features, the swept area and seafloor clearance were measured. These analyses address direct seafloor contact, the proportion of disturbed habitat features, and the effect components have on the shape and height of the footrope.

RAISED FOOTROPE FOR THE EASTERN BERING SEA POLLOCK FISHERY

1.1 INTRODUCTION

The US Alaska pollock fishery is a major contributor to domestic and global fish production and the work reported here addresses an issue this industry faces — developing new trawl designs that efficiently capture pollock near the seafloor, avoid salmon, crab and halibut bycatch, and minimize adverse impacts on benthic habitats. To reduce crab and halibut bycatch, the Alaska pollock fishery is currently required to fish with pelagic trawls (trawls designed to fish mid-water). Pelagic trawls have very large openings created from flying doors and large meshes in the mouth that herd schools of pelagic fish toward the codend. The trawls are designed to be towed in the mid-water where most pelagic fish school (Montgomerie and Forbes 2015). Additionally, the Alaska pollock fishery is restricted from adding any disks, bobbins, rollers, and chafing gear on the footrope, and no flotation devices (50 CFR § 679.24). When a conventional pelagic net is fished mid-water, there is no impact on the seafloor. Adult Alaska pollock (*Gadus chalcogrammus*) aggregate on or near the seafloor, particularly during the day (e.g. Mecklenburg, et al. 2002, Tsuji, S. 1989). A pelagic trawl is not optimal for capturing pollock near the seafloor and can have variable seafloor contact which can increase the potential for benthic impacts.

The Alaska pollock fishing industry, in collaboration with scientists at National Oceanic and Atmospheric Administration (NOAA) Alaska Fisheries Science Center (AFSC) and Alaska Pacific University (APU), has been actively pursuing new trawl designs to address bycatch and seabed contact issues while maintaining a viable pollock capture efficiency. This research quantifies the benthic impacts of modified footrope configurations (one that fits under current regulations and five that do not). Other elements of the broader conservation engineering program, including the development of net designs and research into new halibut and crab bycatch avoidance devices, are underway and sponsored by other collaborating partners, and will not be reported in this thesis.

Initial discussions with pollock fishers indicated that they would continue to use off-bottom doors for all pollock trawling, so this study only examined groundgear added to the footrope. A raised footrope can be achieved with a variety of components, including floating line material, and a range of spacing, weights, and sizes of lifting devices (e.g. bobbins, He 2007). The various configurations selected for this study were designed to systematically contrast the effects of operational parameters, such as footrope height above the seafloor and spacing between tracks of lifting devices. Thus, the amount and degree of seafloor contact with the benthos varies for each alternative configuration.

Essential Fish Habitat (EFH) guidelines are reviewed and updated every five years; the 2015 5-year EFH Review included new models to more precisely estimate habitat impacts and determine their severity. The Magnuson Stevens Fisheries Conservation and Management Act (MSA) requires all fisheries management plans to minimize the adverse impacts of fishing on EFH to the extent practicable (16 U.S.C. 1801). According to the Federal Regulations, an impact is adverse if it is “more than minimal and not temporary in nature” (50 CFR § 600). The 2015 5-year EFH Review describes the updated Fishing Effects (FE) model used to evaluate fishing impacts. The model is used to estimate “undisturbed and disturbed habitat from one time step to the next” by taking into account the location, the type of gear, and the sediment (NPFMC 2016). The recovery calculation takes into account the recovery for each sediment type and for each habitat feature. In a best case scenario these models are useful to managers for determining whether fishing impacts are likely to be more than minimal and not temporary in nature, and the progression of the impacts. Although the gear modifications in this thesis are not evaluated via the FE model, they are evaluated similarly with the nominal, contact-adjusted and susceptibility-adjusted swept areas that are incorporated in the FE model.

Susceptibility is useful when evaluating habitat impacts from mobile fishing gear. Benthic structure-forming geological and biological features may provide shelter for fish or their prey and are vulnerable to adverse impacts from contact with trawl gear components (Grabowski et al. 2014). Therefore, an assessment of EFH vulnerability requires knowledge of the susceptibility and recovery of a structure. In addition to the nominal and contact-adjusted swept areas, susceptibility was incorporated in the swept area analysis; it is defined as the proportion of features encountered by fishing gear that have their "functional habitat value" reduced. Functional value indicates the usefulness of that feature in its intact form to a fish or prey species requiring shelter. Since the functional value of a particular feature is difficult to assess directly and varies by species, the percent reduction in the number of geological or biological features is used as a proxy for reduction in functional value. This analytical framework is common in the gear impacts literature (e.g. Stokesbury and Harris 2006, ICES 2010).

Seafloor clearance is the calculated height of the footrope above the seafloor, which in addition to swept area, is useful in evaluating benthic impacts. The raised footrope modifications were expected to have a varying degree of seafloor clearance and thus have varying impacts on the benthos. The effective lift created by the bobbins can be inferred from previous work on bottom trawls of the groundfish fishery (Rose et al. 2010 a&b), but the effects of materials and lifting elements together is unknown. The estimated seafloor clearance has thus far been determined by buoyancy of the material and dimensions of the bobbins. To quantify seafloor clearance, bottom contact sensors measured height from eleven points along the footrope. Previous studies (e.g. Weinberg 2003, Hannah and Jones 2003) have used bottom contact sensors on the footrope, but only attached at the center. Placing the sensors (Onset Hobo Pendant G Acceleration data loggers) at multiple locations along the footrope provides the ability to determine effective lift of each section and the entire footrope based on the placement of the materials. The seafloor clearance data can also be paired with the biological feature data used for susceptibility analyses to gauge the effect that seafloor clearance has on benthic communities. The objective of this thesis was to quantify habitat impacts of modified raised footrope configurations for a pelagic pollock trawl by measuring swept area and seafloor clearance.

This interdisciplinary, collaborative study has an overall goal of using conservation engineering to address pelagic trawl gear designs that potentially impact EFH in the Eastern Bering Sea (EBS). The Alaska pollock fishing industry, scientists at NOAA AFSC and APU have collaborated to pursue new trawl designs that reduce seabed contact, yet maintain efficient capture of pollock. This research aims to quantify habitat impacts of modified raised footropes for the pelagic pollock trawl.

The objectives were to:

1) test a suite of modified footrope elements designed for lifting the footrope of a pelagic pollock trawl;
2) quantify the habitat impacts of the modified raised footrope configurations; and
3) estimate the seafloor clearance of each modified element.

The swept area framework was used to calculate 1) nominal swept area (A), 2) contact-adjusted swept area (A_c), and 3) susceptibility-adjusted swept area (A_s) for each configuration. Seafloor clearance was estimated from the tilt angle recorded by the bottom contact sensors attached to each footrope configuration at multiple locations. The seafloor clearance measurements allowed for understanding the effects of materials and components on seafloor clearance, as well as the behavior of the entire configuration.

Based on the design of the raised footrope, seafloor contact is expected to decrease as seafloor clearance is increased, therefore, reducing habitat impacts. The contact-adjusted swept area (A_c) and the susceptibility-adjusted swept area (A_s) will be less than the nominal swept area (A). The amount of A_c will vary between the different footrope configurations. The seafloor clearance is expected to be at least 10 cm nearest the bobbins (radius of the bobbins 12.7 cm (5 in) minus the radius of the rope 2.54 cm (≈1 in)) and vary in the mid-span of the sections. The seafloor clearance characteristics of each footrope are expected to be related to the buoyancy of its component materials, with polyethylene rope being the most buoyant, combination rope the heaviest, and Spectra rope neutrally buoyant. When comparing seafloor clearance and impact, susceptibility-adjusted swept area is expected to increase as seafloor clearance decreases. The null hypothesis is that these modified gear configurations have no effective lift and therefore have full contact when trawled on bottom, and that there is no difference between sea whip densities between impact and control areas.

1.2 METHODS

Site Description

From May 19th to June 4th of 2014, field tests were conducted in the EBS (Figure 1). The 46 km^2 study site[1] was chosen based on little to no evidence of fishing activity for at least the past 10 years (author's assessment of vessel monitoring system data), the presence of sea whips

---

[1] Study area corner coordinates: W 55 45.7 N 168 32, W 55 47.7 N 168 32, W 55 45.5 N 168 21, W 55 43.5 N 168 21

(author's assessment of NMFS trawl survey and seafloor camera data), and depths (150 - 175 m) and sediments (mud/ sand with some gravel) similar to those found in EBS pollock fishing areas.

Conventional Pelagic Trawl Net

The footrope configurations were attached and tested on a conventional pelagic pollock trawl with a few minor adjustments to the fishing line. A wide-body, long-wing pelagic trawl constructed by Swan Net USA was used to evaluate the raised-footrope configurations. The conventional footrope was continuous bare chain (1.3 cm sides, 1.6 cm center [1/2 in 2.9 kg/m in seawater, 5/8 in 5.1 kg/m in seawater] Table 1), connected to a 3.8 cm (1.5 in) diameter polyethylene fishing line with 1 m dropper chains every 3 m. One goal for designing the raised footrope was to limit weight, and hence seafloor contact, to a few short portions of the footrope. The conventional chain footrope and droppers were removed, leaving only one chain link attached to the fishing line at each dropper location. Other metal components were removed, including: a chain section in the center of the fishing line (replaced by 3.8 cm (1.5 in) polyethylene rope) and many small steel shackles used to form the belly panel meshes (replaced by twine knots). A few of the steel shackles remained in the lower forward wings. This configuration was held constant across all footropes tested.

Footrope Design

The design of the raised footrope modification is described in detail to explain the attachment and spacing. To construct a light raised footrope that reduces the potential benthic impacts of conventional pelagic trawls fished near the seafloor, the chain footrope (201.8 m, Table 2, Figure 2) was replaced with seven 27.4 m (90 ft) rope sections, separated by six 2.1 m (7 ft) weight sections throughout, and two 1.8 m (6 ft) weight sections on the forward ends (total length 208.5 m, Table 2, Figure 2). The weight necessary to shape the pelagic trawl was concentrated in the conventional weight chains included in the alternative raised footrope. The weight chains were 2.1 m (7 ft) of 1.59 cm (5/8 in) chain, in line with the ropes, with 8 links of 3.81 cm (1.5 in) buoy chain that secured to the in-line chain using three 2.2 cm (7/8 in) hammerlocks. Two additional 2.2 cm (7/8 in) hammerlocks were used to secure the in-line chain to the 27.4 m (90 ft) sections of rope. The overall weight of each weight chain was 93 kg (80 kg in seawater, Table 1, Figure 3). One hollow steel bobbin 25.4 cm (10 in, each bobbin weighs 7.3 kg in saltwater, Table 1, Figure 3) was installed at each end of the weight chain in all but one footrope configuration. The two wing tip weight chains were only 1.8 m (6 ft) to equal the conventional footrope length (201.8 m, Table 2, Figure 2). The footrope was attached to the fishing line of the pelagic net with 1.2 m (4 ft) spectra loops with both ends shackled to the remaining links of the original dropper chains and looped under the footrope (Figure 4). This created 0.6 m (2 ft) of spacing between the fishing line and the footrope. Where these droppers were aligned with one of the weight clusters, the loops were run through the 1.6 cm (5/8 in) chain therefore fixing the location at both footrope and fishing line.

Groundgear Materials

Multiple materials were used to construct the footrope sections, varying by weight, spacing and seafloor clearance. Three types of rope, seen in Figure 5, were alternated amongst the seven 27.4 m (90 ft) sections of the inner wings, outer wings, corners, and center. Combination (“combi”) rope is made of steel cables wrapped in polyethylene fiber with a 5.1 cm (2 in) diameter and has a weight in seawater of 2.2 kg/m (Table 1, Figure 6). Polyethylene rope (“poly”) is made of woven polyethylene fibers with a 5.1 cm (2 in) diameter and is buoyant (-0.026 kg/m in seawater, Table 1, Figure 6). Spectra rope is made of braided ultra-highmolecular-weight (UHMW) polyethylene fibers and has a 1.9 cm (0.75 in) diameter with a 0.047 kg/m in seawater (Table 1, Figure 6). Two alternate combination-rope sections, with additional, mid-span supports were tested. The first bare combi, had no lifting elements, except when used in the center section, where a 25.4 cm (10 in) rubber disk and a 3.8 cm (1.5 in) buoy chain were installed in the center, splitting the section into two 13.7 m (45 ft) intervals (labeled “combi45”, Table 1, Figure 6). The second, “combi30” was a 27.4 m (90 ft) section of combi rope with two 25.4 cm (10 in) rubber disks every 9.1 m (30 ft), creating three 9.1 m (30 ft) intervals (Table 1, Figure 6).

Footrope Configurations

Six unique footrope configurations, labeled as Groundgear 1 through 6 were constructed with varying materials alternated through the seven 27.4 m (90 ft) sections (Table 3, Figure 6). Each of the six footrope configurations was towed twice. All seven rope sections of the Groundgear 1 footrope were constructed of poly rope and the eight 2.1 m (7 ft) long weight sections were configured without bobbins. Groundgear 6 used the same poly rope sections, but had 25.4 cm (10 in) diameter steel bobbins installed on both ends of each weight section. Groundgear configurations 2-5 used mixed materials between the rope sections with different materials alternated through the two outer wings, the two inner wings, the two corners, and the center. All of these configurations had weight sections with bobbins installed. Groundgear 2 (S-C-C30-P) was set up with Spectra in the outer wings, combi in the inner wings, combi30 in the corners, and poly in the center. Groundgear 3 (C-C30-P-S) was set up with combi in the outer wings, combi30 in the inner wings, poly in the corners, and Spectra in the center. Groundgear 4 (C30-P-S-C45) was set up with combi30 in the outer wings, poly in the inner wings, Spectra in the corners, and combi45 in the center. Lastly, Groundgear 5 (P-S-C-C45) had poly outer wings, Spectra inner wings, combi corners, and a center made of combi45.

Experimental Trawling

Experimental trawls occurred along a series of north-south transects (approximately 3.8 km (2.3 mi) long) established at 0.4 longitudinal degree intervals from N 168 25.6 to N 168 31.2. The trawls were towed at typical fishing speed (approximately 3.2 knots) in contact with the seafloor. The transect spacing provided unfished control areas parallel to each transect. Trawl groundgear configurations were randomly assigned to two transect lines each although a reported trawl “hang-up” near the line at N 168 30 eliminated this transect line and the assigned trawl occurred at a different transect (Figure 7). A trawl sonar (Wesmar 770), mounted on the third wire, monitored the shape and position of the trawl mouth relative to the seafloor, confirming that the trawl was on the seafloor throughout all trawls.

Observation Transects

After the experimental trawls were completed their direct seafloor impacts were recorded and observed with a submersible video camera system and a DIDSON sonar unit. The observations of the seafloor were made five to eight days after the experimental towing. Sampling occurred along 10 observation transects which crossed each trawl track and adjacent control area. The observation transects were perpendicular to the experimental trawl tows (heading east and west) and crossed each trawl track and adjacent control area 20 times (two tracks per groundgear configuration and 10 observation transects; Figure 7). Each observation transect was approximately 12 km long.

All of the instruments used for collecting observations were mounted on a mesh panel, of which the buoyancy was adjusted, and then hung parallel to the seafloor across the headline of a

Nor’Eastern bottom trawl towed behind 816.5 kg x 2.7 m (1,800 lb 6x9 ft) V doors. This is the same trawl and doors used in Gulf of Alaska and Aleutian Islands trawl surveys by the Alaska Fisheries Science Center (Stauffer 2004). When towed, the mesh panel was stable and its height was adjustable. Sampling instruments attached to the mesh panel included (from starboard to port): a backup underwater video camera, DIDSON sonar, an altimeter, and the primary underwater video camera (Figure 8). The video cameras were low-light security cameras with Sony EXview 1/3 in CCD chipsets rated at 0.001 lux sensitivity and were equipped with LED illuminators providing over 1,000 lumens from a Cree XP-L cool-white array at 6500 K color temperature. Neutral buoyancy of the panel was achieved by adding one 25.4 cm (10 in) green float to the starboard and port ends of the panel; the backup camera had nine floats (0. 8 kg buoyancy each), the lighter primary camera had two floats, and the altimeter had three floats. The DIDSON, mounted on top in a cage, had four 20.3 cm (8 in) floats and one 25.4 cm (10 in) float (Figure 9).

The layout of the mesh panel and the instruments allowed for each to capture the effects of the experimental groundgear configurations. The DIDSON recorded sonar imagery (1.8 MHz frequency and 8 frames per second) of the seafloor surface while the two cameras below captured video of biological features (30 frames per second with continuous lighting from the LED illuminators). The altimeter monitored the height of panel and therefore the viewing area of each imaging instrument.

Data Collection from Field Observations

After the observation transects were completed, the data from the video and sonar footage were extracted and compiled using computer software. Sound Metrics DIDSON software Version V5.26.06 was used to review the sonar footage, with the intensity set to 75, the threshold to 12, and the platform motion correction parameters were adjusted to enable velocity, manual override, and velocity set to 3 (determined by tow speed). The DIDSON data, allowed the gear tracks (e.g. chain weight and bobbin scars) to be identified and measured (Figure 10). Video from the primary camera was reviewed with VLC Media Player 2.2.1 to identify the tracks and match them to the DIDSON observations. The condition of sea whips was observed and recorded using Video Logger, processing software designed at the AFSC. Playback was kept constant at half speed and the conditions of sea whips were assigned as either up-intact, down, or damaged.

Nominal Swept Area

A concept and equation for nominal swept area was defined to analyze the raised footrope configurations. Nominal swept area has been used to analyze the contact of a typical bottom trawl with five components that could contact the seabed: the doors, clump weights, the sweeps, the footrope, and the net (Figure 11). Since the net follows directly behind the footrope, the two are integrated in the swept area calculation. The raised groundgear configurations in this study were attached to a pelagic trawl and so the doors and bridles (sweeps) did not contact the seafloor. The footrope wings and center sections that did contact the seafloor were treated separately. Thus, for the purposes of this study nominal swept area (A) can be expressed as

1) $A = d_t[(2 \times w_w) + (w_c)]$

where d_t is distance (km) covered in one tow event,

w_w is the effective width (km) of the footrope wing (the outer wing, inner wing, and corner combined),

w_c is the effective width of the footrope center.

While the linear dimensional width of trawl groundgear can be estimated from the gear design specifications, the actual dimensional width of the gear varies along the towpath as due to myriad factors including vessel speed, water depth, and seabed roughness. The nominal swept area (A) of each trawl footrope configuration examined was estimated by measuring the linear width at ten points along each tow path (north and south) and multiplying by the distance towed.

Contact-Adjusted Swept Area

The actual contact of the footrope within the nominal tow path varies with gear design (e.g. lifting elements, buoyant materials), fishing practices, and numerous other factors (e.g. water depth, weather conditions). The contact-adjusted swept area (A_c) is the actual amount of area contacted by the footrope along the towpath and is estimated using component-specific modifiers ("contact indices") which adjust the proportion of contact between 1 (full contact) and 0 (no contact; see Figure 11). The formula for A_c is:

2) $A_c = d_t\,[(2 \times w_w \times c_w) + (w_c \times c_c)]$

where c_w is the contact index of the footrope wing (outer wing, inner wing, and corners

c_c is the contact index for the footrope center.

The contact indices are the proportion of the effective width determined to actually contact the seabed. For example, the trawl used in this study employed pelagic doors which fly above the seabed lifting the bridles (sweeps) as well. As such the doors and bridles have a contact index value of 0 and were dropped from the A and A_c equations.

The contact-adjusted swept area (A_c) was calculated using the contact (c_x) values based on measurements collected using the DIDSON observations. Ten replicate measurements were made on all seabed contact observations detected in the DIDSON imagery (Figure 10). The contact indices used to calculate A_c were estimated by averaging these measurements for each configuration and transect.

After the nominal and contact-adjusted swept areas were calculated, the two were compared. Total nominal swept area (A) and its variability were assessed for each footrope configuration during trawl sets, and haul-backs typical of normal fishing practices. The contact index for each tow and configuration was estimated as the proportional area of seafloor actually contacted by gear components (A_c) divided the nominal area swept (A).

Susceptibility-Adjusted Swept Area

The observed effects on sea whips were converted to a proportion and used to calculate the susceptibility-adjusted swept area. Differences in susceptibility were used to compare footrope configurations using methods similar to those used to compare contact. The maximum potential effect of a trawl tow would occur if all elements of a geological and biological feature in the nominal area (A) of that tow were fully impacted. Component-feature-specific susceptibility indices, defined as the impacted proportion of each sea whip in the area swept by each component, were estimated (Figure 12). A susceptibility-adjusted swept area (A_s) that combines effects of all components by weighting component-specific susceptibilities by component areas was defined as:

3) $A_s = d_t \left[(2 \times w_w \times s_w) + (w_c \times s_c)\right]$

where s_w is the susceptibility index of the footrope wing (outer wing, inner wing, and corner)

s_c is the susceptibility index of the footrope center.

A susceptibility index (A_s/A) was used to estimate the overall susceptibilities of sea whips for each footrope configuration. Differences between the ratios were used to differentiate configurations that have less impact on habitat.

Modeling Swept Area

Empirical measurements of the effective width (km) and contacted width (km) were used to calculate A and A_c for each footrope configuration. The contacted widths were estimated using measurements of the footrope contact marks in DIDSON imagery collected along the ten seabed observation transects across each tow path. Effective width was estimated using the linear distances spanned by the footrope wings (w_w) and center (w_c) as determined using weight cluster tracks observed along the seabed video transects across each tow path. Time and speed information associated with the seabed video observations of these tracks was used to calculate the w_w and w_c distances. Nominal swept area (A) for each configuration was estimated by multiplying effective width by the tow length (Equation 1). The contact index for each footrope section was estimated by determining the proportion of the effective width that contacted the seabed. The A_c was then estimated by multiplying the contact-adjusted effective width by the tow length (Equation 2).

General Linear Mixed Models (GLMMs) implemented in a Bayesian framework were used to test the null hypothesis of no difference between sea whip densities (combined downed and upright) within each pair of adjacent impacted and control areas. This was done to ensure that each pair of areas could be considered true replicates for the purposes of this study. Next, GLMMs were constructed to test the null hypothesis that the proportion of downed or damaged sea whips counted in the adjacent impacted and control areas did not differ for each footrope configuration. Finally, the difference in the proportions of downed versus upright sea whips in impacted and adjacent control sites (estimated as percentages) were used to estimate the susceptibility indices and thus A_s for each footrope configuration (Equation 3).

Separate regressions were run for sea whip density and for downed and damaged sea whips. Density data were collected as counts of individual whips per transect view area (individuals per m^{-2}) and were thus modeled using Poisson GLMMs with inclusion of an over dispersion variance (Appendix A.1). The empirical proportion of downed sea whips within impact and control areas was calculated by dividing the number of downed sea whips by the total number of sea whips observed along each transect. The empirical proportion of damaged sea whips was calculated the same way. Downed and damaged sea whips were treated as binomial processes, constructing binomial GLMMs, whereby the 'size' of each binomial trial within a sampling unit was the total number of whips present, and 'successes' are downed or damaged sea whips (Zuur et al. 2009; Hadfield 2010, 2014). In this manner, the binomial 'probability of success' can be interpreted synonymously as the proportion of downed or damaged sea whips.

Previous work on sea whips showed potential for strong local autocorrelation in sea whip distribution (e.g. Malecha and Stone 2009, Rose et al. 2010 a&b). As a result a hierarchical sampling design (transects within tow paths and control areas) was implemented. Mixed models were considered appropriate given structure of the sampling design and the need to control for potential pseudo-replication associated with replicate transects within impact and control areas. Bayesian implementation was preferred because it allowed for posterior distributions and credibility intervals to be created for the difference in impacted and control areas in the GLMM framework at the level of the response (i.e., differences measured in the proportion of downed sea whip, as opposed to units on the scale of the linear predictor component of generalized regression models). Furthermore, with a Bayesian implementation, parameter estimates could be obtained for data sets with “complete separation,” where for example, sea whips may be absent in sample data from within a control area but present in an adjacent impacted area for a given footrope configuration. Separation issues for discrete data can cause convergence problems with maximum likelihood based model fitting, some of which can be overcome with Bayesian implementation of GLMM models (Gelman et al. 2006).

Regression models for density and proportion of downed or damaged sea whip data were constructed with Reserve (Impact or Control), Gear (Footrope Configuration), and a Reserve by Site interaction as fixed effects, and Track (transects) as a normally distributed random intercept term (Appendix A 2 and 3). This model structure allowed for different reserve effects to be realized between impact and control areas across the footrope configurations tested.

GLMM models that predict the effect of the raised footrope on sea whips were used to predict the significance of gear effects. GLMM models were fit using the 'MCMCglmm' package (Hadfield 2010) in the R statistical programming environment (RCT 2013). Fixed effects priors were specified as multivariate normal priors with large variances following 'MCMCglmm' defaults. It is notable that binomial GLMMs in 'MCMCglmm' by default include an observation level random effect to accommodate over dispersion. All reported model predictions are marginal effects at the level of the response variable (i.e. density, proportion), which include influence of random effects in model predictions (see Atkins et al. 2013 for a good explanation of marginal versus conditional GLMM model interpretation). For the binomial probability models, formulae provided in Hadfield (2014) were used to approximate marginal effects on the response scale (also see Atkins et al. 2013). The difference between impact - and control - area among footrope configurations was calculated as a derived parameter at the level of the response variable. For example, for a given regression, the posterior distribution was generated for the difference between predicted probability of presence of a downed sea whip in the control area minus the predicted probability of presence of a downed sea whip in the impacted area for a given footrope; positive values indicate a positive "reserve" effect on the presence of a downed sea whip in the impacted area, and vice versa (Appendix A.2). Furthermore, by calculating the size of the predicted effect directly, the method integrates over both the statistical (precision of model predictions, inclusive of the random effect structure specified in the model to account for the nested structure of the data) and biological (magnitude of the difference) significance of a given gear effect.

The GLMM regressions were fit with a single MCMC chain run with 100,000 iterations, a 25% thin rate, and a 75,000 burin period (effective sample size = 1000). Trace plots of parameter draws indicated that the models were well mixed, with bell-shaped posterior parameter distributions for all fitted fixed effects and random effect variances (See Appendix).

Estimated Seafloor Clearance

Bottom contact sensors that measured tilt based on acceleration were used to estimate footrope height above the seafloor. The y-axis tilt angles measured from the bottom contact sensors (accelerometers) were converted to height above the seafloor and averaged for component or configuration to estimate seafloor clearance. Each sensor was housed in a rectangular 10.8 x 10.2 x 6.3 cm (4.25 x 4 x 2.5 in) plastic unit fastened to the footrope. A 15.2 cm (6 in) steel rod (1 cm diameter) with three lead weights (2 cm diameter, 3 cm long) extended from the back of each unit causing it to trail behind the footrope when the rod contacted the seabed (Figure 13). At clearance heights greater than 20.3 cm the rod did not contact the seabed and the sensor remained vertically oriented. As such, maximum clearance detectable was 20.3 cm (8 in), the total distance from the bottom of the footrope to the tip of the rod, and these measurements were indicative of the footrope being 20.3 cm or higher above the seafloor. At clearance heights less than 20.3 cm, the sensor tilt increases with decreasing clearance height such that clearance (cm) can generally be estimated as (cos(90° - y°) x 20.3), where y° is the angle of the sensor as it rotates on the footrope.

Bottom contact sensors were placed: 1) on the rope ahead of the third bobbin of both outer wings, 2) at the mid-span point of both inner wings, 3) on the rope ahead of the second bobbin of both inner wings, 4) at the mid-span point of both corners, 5) on the rope ahead of the corner bobbins, and 6) at the mid-span point of the center. The 11 sensors were numbered, assigned to starboard or port, and kept in order for consistency (Figure 14).

The design and placement locations of the bottom contact sensors were taken into considerations when calibrating for height. Due to the orientation of the sensor housing when mounted on the configurations, sensors on the port and starboard sides rotated through different ranges of tilt degrees (82.8° to 0° starboard and 97.2° to 167.2° port) as the groundgear neared the seafloor. Calibration trials were done to determine the relationship between the angles recorded by the accelerometer and clearance heights. Tilt angles were recorded from a bottom contact sensor attached to a simulated footrope set at clearance heights from 20.3 cm to 3.8 cm (8 in to 1.5 in) at 0.64 cm (0.25 in) intervals above the seafloor and the corresponding tilt angles were plotted (Figure 15). Calibrations included both orientations, corresponding to the starboard and port deployments. In the starboard orientation, 82.8° was equal to a height of 20.3 cm (8 in) or higher indicating complete seafloor clearance, and 0° was equal to zero centimeters of clearance, indicating contact with the seafloor. Starboard sensor clearances (cm) were equal to (cos(82.8° - y°) x 20.3). For the port orientation, 97.2° was equal to a height of 20.3 cm (8 in) or higher, and 167.2° was equal to zero centimeters, indicating seafloor contact. Port side sensor clearances (cm) were equal to (cos(97.2° - y°) x 20.3). The calibration experiments indicated that sensor tilt was a strong predictor of clearance height (R^2 = 0.96) for both sensor orientations

(Figure 15). Mean seafloor clearance values and range were estimated and plotted for each sensor (representing a component and material type) on each footrope configuration. Analysis of Variance (ANOVA) was used to compare the mean clearance estimates by footrope configuration, sensor location and wing and center material type. The measured clearance was also compared to the anticipated clearance based on the buoyancy of the rope material and diameter of the lifting elements (Table 4).

Fishing Practicality

Changing from a footrope with continuous chain to one with widely-spaced weighted sections and bobbins raised concerns that handling the net during deployment and retrieval would be more difficult, particularly the potential for tangling in the large meshes of the trawl net. Fishing practicality was tested via observations of on-deck handling and net shape once deployed. The interaction of the crew with the net as if fishing was observed and recorded with cameras set up at different points on deck. We looked for evidence of delay, tangling or hazards associated with the footrope. The shape of the trawl opening, as indicated by the net mensuration sonar, was examined for normal height, width, and seafloor proximity.

1.3 RESULTS

The nominal swept area, bottom contact, impact to sea whips and clearance heights of six raised footrope configurations were quantified using direct observations of the seabed after trawling and via bottom contact sensors. The raised footropes had comparable nominal swept areas (0.3 km^2) with little bottom contact for all configurations (A_c/A less than about 0.05) with clearance averaging between 10 and 16.6 cm between contact points. About 7% more sea whips were downed and 2% more were damaged in impacted areas relative to the control areas. Although footrope clearances only as high as the radius of the lifting elements (10 cm) and footrope radius were anticipated, greater clearance heights were often measured. Overall, clearances above 12.7 cm (5 in) occurred for 61% of the component measurements. The footropes constructed completely of poly rope had the highest clearance heights, the lowest contact-adjusted swept area, and the lowest proportion of downed and damaged sea whips.

Nominal Swept Area

The nominal swept area varied little between tows and had a mean area of 0.329 km^2 (Min. = 0.273 km^2, Max. =0.420 km^2, SD=0.075, Table 6) with differences attributable to variations in effective widths (Figure 16).

Contact-Adjusted Swept Area

Contact-adjusted swept area (A_c) varied among footrope configurations, but was small for all configurations (2-16% of A; Table 5, Figure 17). Groundgear 1, with all poly rope sections and no bobbins, had the lowest A_c values (0.002 km^2 and 0.005 km^2) of all gears. This result ran contrary to expectations as it had no bobbins. Groundgear 6, with all poly rope sections with bobbins, had the next lowest A_c value (0.007 km^2), but showed substantial variability with A_c nearly double (0.013 km^2) for one of the trawls. The mixed configuration footropes (Groundgear 2-5) had more contact-adjusted swept area (0.011 - 0.017 km^2) and higher contact ratios (A_c/A = 3.3 - 5.5%) than the all poly rope configurations. While the differences were small, it is notable that for Groundgear 2 (S-C-C30-P) and 3 (C-C30-P-S), configurations with 4 sections of combination wire had the highest A_c and A_c/A estimates of all the footropes tested (0.017 km^2, 5.5% and 0.016 km^2, 5.5% respectively, Table 5).

Sea Whip Density

The density of sea whips in the adjacent control and impact areas were comparable and did not skew the analyses of downed and damaged sea whips. About 25,000 sea whips were observed in the study area, and median whip densities ranged from 0.13 to 0.52 individuals per m^{-2}, but were similar in the control (0.22 sea whips per m^{-2} with 95% credibility intervals ± 0.06) and impact areas (0.24 sea whips per m-2, with 95% credibility intervals ± 0.05) (Table 6). The differences in median sea whip densities in the impact and adjacent control areas for each footrope configuration were very small, ranging between -0.08 to 0.08 sea whips per m^{-2}, with overlapping 95% credibility intervals in all cases. Therefore, the control and impacted areas could be treated as replicates for the purposes of downed and damaged sea whip analyses (Figure 18).

Susceptibility-Adjusted Swept Area-Downed Sea Whips

For each of groundgear configuration, there were a higher proportion of downed sea whips in the impact area compared to the adjacent control area. Overall, 7.4% more sea whips were predicted to be downed in the impact areas (18.1%), compared to the control areas (10.7%). However, of the 12 comparisons made between impact and control pairs, differences in the proportion of downed sea whips were statistically significant (i.e. 95% credibility intervals for predicted downed sea whips did not overlap) for only one impact and control pair (one tow with Groundgear 2; Table 7, Figure 19). Groundgear 6, with all poly rope and bobbins, had the smallest differences of predicted downed sea whips in the impact and control areas, 2% (±2.2%) and 4% (±2.4%), respectively, followed by Groundgear 1, with all poly rope and no bobbins, with a predicted difference of 3% (±1.9%) and 5% (±2.4%), respectively. The mixed configuration footropes (Groundgear 2-5) showed predicted differences between impact and control areas that ranged between 4 and 16%. Notably, Groundgear 2 (S-C-C30-P) and 3 (C-

C30-P-S) had the greatest differences in predicted downed sea whips (16% and 13%, respectively) and showed the most variability between tows. These results coincide with the expectations of the gear being the two heaviest configurations due to four sections of combi rope. The predicted percentages of downed sea whips were used to estimate the susceptibility-adjusted swept area for each footrope configuration (Table 8).

Susceptibility-Adjusted Swept Area-Damaged Sea Whips

Damaged sea whips occurred less than downed sea whips, so the results were less definitive than the results for downed sea whips. Only 405 of the 24,859 sea whips observed were damaged and the median predicted percentage of damaged sea whips in the impacted areas was 2.8% (± 0.004%) greater than in the control areas (0.6%). There were a few tracks, however, with a significant difference between the adjacent control and impact areas. In all cases, the predicted percentage of damaged whips was higher in the impact versus control area for each footrope configuration, and 4 of the 12 impact and control comparisons were significantly different (Groundgear 1, 2, 3, and 5; Table 9, Figure 20). Interestingly, in these four cases only one of two replicate comparisons showed a significant difference.

Seafloor Clearance

Seafloor clearance was first measured as the average height above the seafloor for each component location along the footrope. The bottom contact sensors collected data at six-second intervals from 11 locations across each groundgear configuration. Average clearances from each sensor location of each tow (11x6x2) were calculated; averages were selected to smooth out the noise in the data caused by other factors such as flow causing the sensors to swing or bounce. A few exceptions occurred when a sensor malfunctioned or when a sensor housing was apparently tangled, producing out-of-range tilts throughout an entire tow. In total, 117 average seafloor clearance estimates were obtained from all six configurations. Only 18% of these were less than or equal to 10.2 cm (4 in) and just 7% were less than or equal to 7.6 cm (3 in) off bottom (Figure 21).

Next, the average seafloor clearance was estimated for each track and component, combined by groundgear configuration, and then plotted with variation described by the range of heights (Figure 22). Seafloor clearance of the configurations ranged from 10.9 cm (4.3 in) to 20.2 cm (8.0 in or more). Groundgear 4 had the greatest seafloor clearance with 18.4 cm (7.2 in, min=15.9 cm, max=20.3 cm) and 20.3 cm (8.0 in or more, min=20.1 cm) above the seafloor. Groundgear 6, the configuration of all poly rope sections and bobbins, had the second greatest clearance of 16.5 cm (6.5 in, min=10.6 cm, max=20.3 cm) and 16.0 cm (6.3 in, min=11.4 cm, max=19.8 cm) above the seafloor. The remaining configurations, Groundgear 1, 2, 3, and 5, had an average seafloor clearance greater than or equal to 10.9 cm (4.3 in) which is at least half of the measurable distance to the seafloor.

To understand material and component effects, the data were arranged by material and component as seen in Figure 23. The seafloor clearance of the 3rd bobbin was consistent for all material types. The poly rope had a lifting effect on the 2nd bobbin, more so than any other material type. The corner bobbin had the greatest lift from Spectra in the corner component. The mid-span components with Spectra were lifted above 17 cm. Finally, six of the twelve center components were lifted above the seafloor more than 14 cm (5.9 in) , and the other half had 7.7 to 10.7 cm (3.0 to 4.3 in) of seafloor clearance.

Finally, seafloor clearance was compared between tracks and by individual component performance to the anticipated clearance (Figure 24). The combi30 and combi ropes were always ahead of the poly rope sections except when poly was in the outer wing. For two of the three configurations in which poly rope was behind combi rope, the poly rope mid-span was possibly weighed down and therefore had less seafloor clearance. The outer wing components were also observed to have a seafloor clearance greater than 12.7 cm (5 in) except for track 5 where it dropped below 5 cm (2 in).

Fishing Practicality

Handling the trawl net with the raised footrope attached did not pose major concerns when deployed and retrieved conventionally by the crew. The trawl net came on and off the reel smoothly once the crew was accustomed to working with it. During haul-backs, additional care was required to keep tension on the groundgear as weight sections passed onto the net reel, to prevent them dropping down as they passed the top of the reel. The groundgear could not be wound as tight on the reel as for a conventional pelagic trawl and the weight sections had a greater tendency to swing once off of the reel, although they did not tangle in the large meshes. Once the trawl net was in the water, there were no groundgear hang ups and the trawl took normal shape at depth. The opening of the trawl was 100 m wide, 14-18 m high according to the net mensuration sonar (Figure 25).

1.4 DISCUSSION

The raised footrope configurations examined here had little bottom contact and achieved greater than expected seafloor clearance. Reducing seafloor contact resulted in low levels of downed and damaged sea whips. The contact- and susceptibility-adjusted swept area analyses were useful tools to quantify habitat impact and the effects on sea whips caused by each groundgear configuration. Seafloor clearance sensors across the entire footrope show potential to provide better understanding of seafloor contact as opposed to a single sensor at the center of the footrope, as done during resource assessment surveys (e.g. Stauffer 2004). Such extensive instrumentation can improve the understanding of interactions between the groundgear components in terms of seafloor contact. The clearance data could also be useful for identifying corresponding seafloor areas in the DIDSON data, and so allow for a comparison of seafloor effects between the sections of mixed groundgear. While the results indicated greater clearance than anticipated, there are many questions and analyses left to address.

The variation of non-chain footrope materials and the few added lifting elements reduced seafloor contact by 95-97%, although potential changes in catch and subsequent effects must still be determined. The gear modifications concentrated the weight of the groundgear into a few short sections of weighted chain, appearing to change the bottom-tending dynamics of the gear. A majority of the evaluations revealed that the groundgear lifted away from the seafloor more than anticipated. Modified footropes were successfully raised by the varying components and could be a useful approach to reducing constraints on the pollock fishery.

In this study, experimental groundgear sections of all raised footrope configurations were successfully raised up off the seafloor. The overall results supported the hypothesis that lighter groundgear materials produce minimal seafloor contact. For example, the heaviest groundgear configurations with four sections of combi rope had only 3.3-5.5% of seafloor contact, the lightest configurations, with only poly rope, ranged from 0.5- 4.0%. Quantifying the impact of these raised footrope designs revealed that most of the length of the groundgear had minimal amounts of seafloor contact and thus minimal impacts to benthic features. This is supported by our analysis of sea whips, used as a proxy for benthic features. There were minimal differences in the number of downed sea whips between impact and control areas.

Using an alternate material that is strong but lighter than bare chain and concentrating the weight into short sections is a simple modification that meets the standards of current regulations. Some concerns remain to be addressed, including the maneuverability of the modified gear while fishing, pollock capture efficiency, and bycatch rates. The modified footropes were not directly compared to conventional pelagic gear in this study.

Changing from a pelagic net with a continuous, bare-chain footrope to one with few widely-spaced weight clusters and bobbins raised concerns among the industry that handling the net during deployment and retrieval would be more difficult. The raised groundgear was easily handled, and the large front meshes did not cause hang-ups on the reel, even while setting rapidly. The weight clusters are still a safety concern when coming off the net reel, as they can drop from the reel if tension is not maintained. More research is needed to support the use of the bobbins used in this study; they show potential for increasing seafloor clearance and minimizing bottom contact.

Management and Policy Implications

This study demonstrates that large reductions in pollock-trawl bottom contact and associated impacts to benthic organisms can be gained by modifying trawl groundgear to include lifting elements (e.g. bobbins) and more buoyant materials. Some of these simple gear modifications could be implemented under current management, while those including bobbins would require changes to regulations. Substantial work is required to explore the efficacy of these modifications for target species catch and bycatch. This research provides encouraging results that demonstrate the potential for major reductions in the benthic interactions of one of the largest and most prolifically fished gears in the Bering Sea (Rose et al. 2010 a&b). Further, the analytical framework used in this project aligns with previous and ongoing work by NOAA

AFSC Resource Assessment Conservation Engineering Division, NOAA-AFSC-Habitat Conservation Division and the North Pacific Fisheries Management Council to assess the effects of fishing on EFH.

GENERAL DISCUSSION

The scope and concentration of disturbance to benthic features can influence the structure and function of benthic features and the quantity and quality of benthic habitat features influences fish population dynamics (Thrush and Dayton 2002). Simple gear modifications like the ones investigated in this thesis are versatile means to mitigate adverse impacts on benthic features, especially for mobile fishing gears which contact the seabed. Fine adjustments, such as replacing chain with lighter ropes or adding lifting elements, are effective ways to achieve groundgear lift and can be made incrementally allowing fishers to optimize seabed clearance without compromising gear catch performance.

Three characteristics of a successful gear modification are 1) reduced seafloor contact, 2) similar or improved catch per unit effort (CPUE), and 3) similar or increased practicality of use as the conventional gear (Rose et al. 2010b). Reduced seafloor contact presumes reduced gear-habitat feature interaction. Multiple methods exist to empirically evaluate contact and gear-habitat interactions. Employed correctly, a combination of swept area analyses, sea floor clearance measurements, and an impact-control study design can definitively show whether a gear modification successfully reduces seafloor contact. For example, the footrope groundgear configurations in this study showed a 95-97% reduction from nominal seafloor contact and only a 2.4-16.1% increase in sea whip interactions compared to control areas.

Swept area analyses are effective means of quantifying reduction in seafloor contact of a gear design compared to nominal contact. Such analyses have been successfully used by two fisheries management councils (NEFMC 2011, NPFMC 2016). When comparing multiple gears that have small adjustments to a primary component (i.e. different configurations of groundgear), these analyses are potentially limited. For example, this study used video and acoustic imagery to calculate swept areas, and it was often impossible to match scars with individual elements (e.g. bobbins, clump weights, etc.). Given this limitation, comparison of whole configurations is possible with swept area analyses, but comparison of the effects of individual elements is not.

The attachment of bottom contact sensors to multiple locations along a single footrope is novel for determining seafloor clearance. Previously, a single sensor was placed in the center of the footrope (e.g. Hannah and Jones 2003, O'Neill and Ivanović 2016, Somerton and Weinberg 2001). With more trials and analyses, the sensor data could be fine-tuned enough to compare the effects of different placements of materials along the footrope. Further, as technology for these sensors improves, the application of bottom contact sensors can extend far beyond seafloor clearance measurements. Some additional applications include furthering the understanding of gear behavior during fishing events and giving fishermen real time seafloor interaction information while fishing.

Control-impact study designs are common to compare impacts of different fishing gear designs (Guyonnet et al. 2008, Rose et al. 2010a&b). These designs can be limited because the patchy spatial distribution of benthic structures makes true replication of impact vs. control sites difficult. In addition, this distribution results in local autocorrelation which can reduce the power of statistical analyses or present challenges to correctly estimating variances about impacts. Directly testing the density of sea whips in the paired impacted and adjacent control areas and then assessing impacts between the two using a General Linear Mixed Model (GLMM) cast in Bayesian framework addresses these limitations.

Gear modifications have strong potential to mitigate adverse fishing impacts, but little empirical work has been done to date. In addition to gear modifications, NRC (2002) also identified spatial closures and harvest limits as tools to minimize fishing impacts. Spatial closures are currently the most widely used mitigation technique in the United States. The state of fish-fishing-habitat science is still in its infancy (Kaiser et al. 2016, Nimick and Harris in Press, Grabowski et al. 2014), and without sufficient scientific information supporting a closure, there can be unintended consequences to such closures simply because of the dynamic and mobile nature of fish and fishing. In contrast, these knowledge gaps do not need to be filled to have a positive habitat effect from gear modifications. If a gear modification successfully reduces sea floor contact, it can safely be assumed that reduced seafloor contact equates to lessened fishing impacts. Gear modification research is costly but critical to balancing habitat conservation and fishermen's livelihood.

This study demonstrates that large reductions in pollock-trawl bottom contact and associated impacts to benthic organisms can be gained by modifying trawl groundgear to include lifting elements (e.g. bobbins) and more buoyant materials. This research provides encouraging results that demonstrate the potential for major reductions in the benthic interactions of one of the largest and most prolifically fished gears in the Bering Sea (Rose et al. 2010 a&b).

REFERENCES

16 U.S.C. Part 1801, U.S. Department of Commerce, National Oceanic and Atmospheric Administration, and National Marine Fisheries Service, Section 2: Findings, Purposes, and Policy, Magnuson Stevens Fishery Conservation and Management Act. P.L. 94-265/ May 2007.

16 U.S.C. Part 1802, U.S. Department of Commerce, National Oceanic and Atmospheric Administration, and National Marine Fisheries Service, Section 3: Definitions; Magnuson Stevens Fishery Conservation and Management Act. P.L. 94-265/ May 2007.

16 U.S.C. Part 1853, U.S. Department of Commerce, National Oceanic and Atmospheric Administration, and National Marine Fisheries Service, Section 303: Contents of Fishery Management Plans; Magnuson Stevens Fishery Conservation and Management Act. P.L. 94-265/ May 2007.

16 U.S.C. Part 1855, U.S. Department of Commerce, National Oceanic and Atmospheric Administration, and National Marine Fisheries Service, Section 305: Other Requirements and Authority, Magnuson Stevens Fishery Conservation and Management Act. P.L. 94-265/ May 2007.

16 U.S.C. Part 1881c, U.S. Department of Commerce, National Oceanic and Atmospheric Administration, and National Marine Fisheries Service, Section 404: Fisheries Research; Sustainable Fisheries Act. P.L. 104-297/ October 1996.

16 U.S.C. Part 1881c, U.S. Department of Commerce, National Oceanic and Atmospheric Administration, and National Marine Fisheries Service, Section 404: Fisheries Research; Magnuson Stevens Fishery Conservation and Management Act. P.L. 94-265/ May 2007.

50 CFR § 648, Fisheries of the Northeastern United States; Atlantic Sea Scallop Fishery; Amendment 10, USA Federal Register Vol. 69, No. 38 / 26 February 2004.

50 CFR § 600.815 Fishery Conservation and Management. Essential Fish Habitat (EFH), USA Federal Register. Vol.67, No.12 / 17 January 2002.

50 CFR § 679.24, Fisheries of the Exclusive Economic Zone off Alaska; Management Measures; Gear Restrictions, USA Federal Register Vol. 80, No. 235 / 8 December 2015.

[AFSC] Alaska Fishery Science Center. (2015) List of Essential Fish Habitat Projects. <http://www.afsc.noaa.gov/HEPR/docs/EFH%20Research%20projects%202015.pdf>. Accessed 10/01/15.

[APA] At-sea Processors Association. (2016) Home page. <http://www.atsea.org/index.php> Accessed 11/30/2016.

Atkins, D.C., et al. (2013) A tutorial on count regression and zero-altered count models for longitudinal substance use data. Psychology of Addictive Behaviors, 27:166-177

Brewer, D., et al. (1996) Assessment of an environmentally friendly semi-pelagic fish trawl. Fisheries Research 26:225-237.

Brodeur, R.D. (2000) Habitat-specific distribution of Pacific ocean perch (*Sebastes alutus*) in Pribilof Canyon, Bering Sea. Continental Shelf Research 21:207-123.

Collie, J.S., et al. (2000) A quantitative analysis of fishing impacts on shelf-sea benthos. Journal of Animal Ecology 69:785-798.

Eagleton, M. and D. Evans (2014) 2015 EFH Review-Approach: Review and Revision of EFH Components within the Council's Fishery Management Plans, and Prioritization of Stocks for Habitat Assessment. North Pacific Fisheries Management Council. Item D-2.

[FAO] Food and Agriculture Organization of the United Nations (2016) The State of World Fisheries and Aquaculture 2016. Contributing to food security and nutrition for all. Rome. 200pp.

Favorite, F. and T. Laevastu. (1981) Finfish and the environment. In Hood, D.W. and J.A. Calder (eds.): The EBS shelf: oceanography and resources, Vol. 1. Univ. of Washington Press, Seattle, Washington: 597-610.

Fishwatch. (2014) Alaska Pollock. <http://www.fishwatch.gov/seafood_profiles/species/pollock/species_pages/alaska_pollock.htm>. Accessed 10/03/15.

Gelman, A., (2006) Prior distributions for variance parameters in hierarchical models. Bayesian Analysis, 3:515-533.

Grabowski, J. H., et al. (2014) Assessing the vulnerability of marine benthos to fishing gear impacts. Reviews in Fisheries Science. 22(2): 142–155.

Guyonnet, B., et al. (2008) Modified otter trawl legs to reduce damage and mortality of benthic organisms in North East Atlantic fisheries (Bay of Biscay). Journal of Marine Systems 72:2-16.

Hadfield, J.D. (2010) "MCMC methods for Multi–response Generalized Linear Mixed Models: The MCMCglmm R Package." Journal of Statistical Software, 33(2), 1–22.

Hadfield, J. (2014) MCMCglmm course notes. Vignette to accompany R package 'MCMCglmm', R Foundation for Statistical Computing, Vienna, Austria.

Hannah, R.W. and S.A. Jones (2003) Measuring the height of the fishing line and its effect on shrimp bycatch in an ocean shrimp (Pandalus jordani) trawl. Fisheries Research 60:427-438.

Hanson, J. and M. Eagleton (2015) Essential Fish Habitat-EFH: An introduction to EFH: regulatory authority, descriptions, 5-year review, HAPC, and consultations. NOAA Fisheries Alaska Region.

He, P., (2007) Technical measures to reduce seabed impact of mobile fishing gears in Kennelly, S. J. (Ed) By-catch Reduction in the World's Fisheries Springer Netherlands. 141-179.

He, P. and Winger P.D. (2010) Effect of Trawling on the Seabed and Mitigation Measures to Reduce Impact. In He P (ed.). Behavior of Marine Fishes: Capture Processes and Conservation Challenges. Blackwell Publishing Ltd., Ames, Iowa. pp. 295-314.

Honkalehto, T., et al. (2008) Results of the echo integration-trawl survey of walleye pollock (*Theragra chalcogramma*) on the U.S. and Russian Bering Sea shelf in June and July 2007. National Marine Fisheries Service NMFS-AFSC-190.

ICES (2010) Spatial methods for comparing and summarizing fish and fish community distributions in relation to environment and habitat. Section 4 In International Council for the Exploration of the Sea. Report of the Working Group on Fish Ecology (WGFE). Sete, France. September 2010.

Jennings, S. and M. J. Kaiser (1998) The effects of fishing on marine ecosystems. Adv Mar Biol 34:201–352.

Kaiser, M.J., et al. (2006) Prioritization of knowledge-needs to achieve best practives for bottom trawling in relation to seabed habitats. Fish and Fisheries 17:637-663.

Krieger, K.J. (1992) Distribution and abundance of rockfish determined from a submersible and by bottom trawling. Fishery Bulletin 91:87-96.

Livingston, P.A. and S. Tjelmeland. (2000) Fisheries in boreal ecosystems. In: ICES Journal of Marine Science. p. 57. In National Marine Fisheries Service 2001(a).

Malecha, P. and R. Stone. (2009) Response of the sea whip (*Halipteris willemoesi*) to simulated trawl disturbance and its vulnerability to subsequent predation. Marine Ecology Progress Series. 388:197-206.

Marine Stewardship Council. (2014) Fisheries Certification Requirements. Marine Stewardship Council V2.0.

McConnaughey, R.A., and K.R. Smith. (2000) Associations between flatfish abundance and surficial sediments in the eastern Bering Sea. Canadian Journal of Fisheries and Aquatic Sciences 57:2410-2419.

Mecklenburg, C., T. and L. Thorsteinson. (2002) Fishes of Alaska. American Fisheries Society, Bethesda, Maryland, US. pp 1037.

Miller, R.J., et al. (2012) Structure-forming corals and sponges and their use as fish habitat in Bering Sea submarine canyons. PLoS ONE 7(3):e33885.

Montgomerie, M. and R. Forbes (2015) Basic Fishing Methods: A comprehensive guide to commercial fishing methods. SEAFISH. Edinburgh, UK.

[NEFMC] New England Fishery Management Council. (2011) The Swept Area Seabed Impacts (SASI) Model: A tool for analyzing the effects of fishing on Essential Fish Habitat. Draft version dated 21 January 2011. 303pp.

[NMFS] National Marine Fisheries Service (2004) NOAA Protocols for fisheries acoustics surveys and related sampling: Appendix 2 for the Alaska Fisheries Science Center. 15 January 2004.

[NMFS] National Marine Fisheries Service. 2005, Final Environmental Impact Statement for Essential Fish Habitat Identification and Conservation in Alaska: Appendix B Table B. 2-4.

[NMFS] National Marine Fisheries Service. 2014. Canyons Corals, and Sustainable Fishing in the Bering Sea. <http://www.nmfs.noaa.gov/stories/2014/06/6_03_14faq_bering_sea_canyons.html>. Accessed 10/02/15.

[NMFS] National Marine Fisheries Service. 2015. 40 years of the Magnuson-Stevens Act. <http://www.nmfs.noaa.gov/stories/2015/11/msa40.html>. Accessed 2/22/16.

[NMFS] National Marine Fisheries Service. 2016. Fisheries of the United States, 2014 <https://www.st.nmfs.noaa.gov/commercial-fisheries/fus/fus14/index>. Accessed 12/6/2016.

[NPFMC] North Pacific Fishery Management Council. 2010. Essential Fish Habitat (EFH) 5-year Review for 2010. Final Summary Report. April 2010.

[NPFMC] North Pacific Fishery Management Council. 2015 Fishery Management Plan for Groundfish of the Bering Sea and Aleutian Islands Management Area: Executive Summary.

[NPFMC] North Pacific Fishery Management Council. 2016. Methods to evaluate the effects of fishing on Essential Fish Habitat: Proposal from the SSC subcommittee. Draft version dated 16 September 2016. 2pp.

[NPRB] North Pacific Research Board. 2015. Bering Sea and Aleutian Islands page. <http://www.nprb.org/nprb/explore-the-science/by-geography/bering-sea-aleutian-islands>. Accessed 10/01/15.

NRC (2002) Effects of trawling and dredging on seafloor habitat. National Research Council, Committee on Ecosystem Effects of Fishing. Washington, D.C., National Academy Press. 136p.

O'Neill, F.G and A. Ivanović (2016) The physical impact of towed demersal fishing on gears on soft sediments. ICES J. Mar.Sci. 73(1):i5-i14.

[RCT] R Core Team (2013) R: A language and environment for statistical computing. R Foundation for Statistical Computing, Vienna, Austria. URL http://www.R-project.org/.

Rose, C.S., et al. (2010a) Effective herding of flatfish by cables with minimal seafloor contact. Fishery Bulletin 108:136-144.

Rose, C.S., et al. (2010b) Cooperative research to reduce the effects of Bering Sea flatfish trawling on seafloor habitat and crabs. AFSC Quarterly Report JanFebMar2010:1-6.

Ryer, C.H., et al. (2004) Behavioral mechanisms underlying the refuge value of benthic habitat structure for two flatfishes with differing anti-predator strategies. Marine Ecology Progress Series 268:231-243.

Sigler, M. F., et al. (2012) Alaska Essential Fish Habitat Research Plan: A research plan for the National Marine Fisheries Service's Alaska Fisheries Science Center and Alaska Regional Office. Processed Report.

Somerton, D.A. and K.L. Weinberg. (2001) The effect of speed through the water on footrope contact of a survey trawl. Fisheries Research. 53(1):17-24.

Somerton, D.A. and C.T. Glendhill (editors). (2005) Report of the National Marine Fisheries Service Workship on Underwater Video Analysis. U.S. Department of Commerce, NOAA Technical Memorandum. NMFS-F/SPO-68-69p.

Stauffer, G. (2004) NOAA protocols for groundfish bottom trawl surveys of the nation’s fishery resources. NOAA Tech. Memo. NMFS-F/SPO-65, 205 p

Stokesbury, K.D.E. and Harris, B.P. (2006) Impact of a limited fishery for sea scallop, *Placopecten magellanicus*, on the epibenthic community of Georges Bank closed areas, Marine Ecology Progress Series. 307:85-100

Stoner, A.W. and R.H. Titgen. (2003) Biological structures and bottom type influence habitat choices made by Alaska flatfishes. Journal of Experimental Marine Biology and Ecology 292:43-59.

Thrush, S.F. and P.K. Dayton. (2002) Disturbance to marine benthic habitats by trawling and dredging: implications for marine biodiversity. Annual Review of Ecology and Systematics 33:449-473.

Tsuji, S. (1989) Alaska pollock population, *Theragra chalcogramma*, of Japan and its adjacent waters, 1: Japanese fisheries and population studies. Mar. Behav. Physiol. 15: 147–205.

Valdemarsen, J.W. and Suuronen P (2001) Modifying fishing gear to achieve ecosystem objectives. Reykjavik Conference on Responsible Fisheries in the Marine Ecosystem. Reykjavik, Iceland.

Wassenberg, T.J., et al. (2002) The impact of fish trawls on megabenthos (sponges) on the north-west shelf of Australia. Fisheries Research. 58:141-151.

Watson, R., et al. (2006) Fishing gear associated with global marine catches: II. Trends in trawling and dredging. Fisheries Research 79:103-111.

Weinberg, K.L. (2003) Change in the performance of a Bering Sea survey trawl due to varied trawl speed. Alaska Fishery Research Bulletin 10(1): 42-49.

Winger, P.D., et al. (2010) Fish Behavior near Bottom Trawls. In He P (ed.). Behavior of Marine Fishes: Capture Processes and Conservation Challenges. Blackwell Publishing Ltd., Ames, Iowa. pp. 67-103.

Zuur, A.F., et al. (2009) Mixed effects models and extensions in ecology with R, Springer, New York.

TABLES

Table 1. The diameter, length, and weight in seawater of conventional and modified components. The symbols correspond to figures are included.

Rope	Diameter (in)	Diameter (cm)	Length (ft)	Length (m)	Weight in Seawater (kg)	Symbols in Figures
Conv. chain footrope	1/2	1.3	662	201.8	510.8	
Conv. footrope center	5/8	1.6	80	24.4	104.6	
Conv. mid-span weight clusters	5/8	1.6	7	2.1	80.0	
Conv. end weight clusters	5/8	1.6	6	1.8	71.2	
poly	2	5.1	90	27.4	-0.712	
Spectra	3/4	1.9	90	27.4	1.29	
combi	2	5.1	90	27.4	60.3	
combi30	2	5.1	90	27.4	≈60.3	
combi45	2	5.1	90	27.4	≈60.3	
Steel bobbin	10	25.4	x	x	7.3	
Rubber disk	10	25.4	x	x		
Weight chain	5/8	1.6	7	2.1	80	
Sensor	x	x	0.66	0.20	0.8	

Table 2. The length and combined weight in seawater (kg) with and without sensors by experimental gear and track.

Experimental Gear ID	Track	Length (m)	Combined Seawater Weight (kg)	Combined Seawater Weight with Sensors (kg)	% Weight Added by Sensor
Groundgear 1	7	208.5	628.7	637.5	1.4%
	11	208.5	628.7	637.5	1.4%
Groundgear 2	8	208.5	967.7	976.5	0.9%
	14	208.5	967.7	976.5	0.9%
Groundgear 3	5	208.5	965.7	974.5	0.9%
	10	208.5	965.7	974.5	0.9%
Groundgear 4	1	208.5	906.7	915.5	1.0%
	12	208.5	906.7	915.5	1.0%
Groundgear 5	4	208.5	906.7	915.5	1.0%
	13	208.5	906.7	915.5	1.0%
Groundgear 6	3	208.5	730.9	739.7	1.2%
	9	208.5	730.9	739.7	1.2%

Table 3. Features and experimental track identification numbers of the six experimental gear configurations.

Experimental Gear ID	Track	Configuration (Outer Wing-Inner Wing-Corner-Center)
Groundgear 1	7 & 11	poly without bobbins
Groundgear 2	8 & 14	Spectra-combi-combi30-poly
Groundgear 3	5 & 10	combi-combi30-poly-Spectra
Groundgear 4	1 & 12	combi30-poly-Spectra-combi45
Groundgear 5	4 & 13	poly-Spectra-combi-combi45
Groundgear 6	3 & 9	poly with bobbins

Table 4. Anticipated lift and seafloor contact of the experimental gear configurations.

Experimental Gear ID	Estimated Lift (in) Configuration	Degree of Seafloor Contact
Groundgear 1	≈2 poly without bobbins	High
Groundgear 2	3 90 ft bobbin spacing, 4 sections of combi	Moderate
Groundgear 3	3 90 ft bobbin spacing, 4 sections of combi	Moderate
Groundgear 4	3 90 ft bobbin spacing, 3 sections of combi	Low
Groundgear 5	3 90 ft bobbin spacing, 3 sections of combi	Low
Groundgear 6	3 poly with bobbins 90 ft spacing	Very Low

Table 5. Nominal (A) and contact-adjusted swept area (A_c) by experimental gear and track.

Experimental Gear ID	Track	Nominal Swept Area (km2)	Contact-Adjusted Swept Area (km^2)	Ratio A_c/A
Groundgear 1	7	0.337	0.002	0.5%
	11	0.337	0.005	1.4%
Groundgear 2	8	0.308	0.017	5.5%
	14	0.324	0.011	3.3%
Groundgear 3	5	0.354	0.012	3.4%
	10	0.297	0.016	5.5%
Groundgear 4	1	0.273	0.013	4.9%
	12	0.333	0.015	4.4%
Groundgear 5	4	0.331	0.011	3.4%
	13	0.320	0.015	4.6%
Groundgear 6	3	0.313	0.013	4.0%
	9	0.420	0.007	1.6%

Table 6. Predicted sea whip densities (downed and upright combined) by experimental gear and track.

Note: Predicted sea whip densities cannot be considered different with a high level of confidence, so tracks may be considered as replicated evaluations of susceptibility-adjusted swept area.

		Sea Whip Density (individuals per m^{-2})			
Experimental Gear ID	Track	impact	control	% Difference	95% CI
Groundgear 1	7	0.21	0.18	3.3%	± 0.275
	11	0.18	0.14	3.6%	± 0.235
Groundgear 2	8	0.21	0.18	2.6%	± 0.895
	14	0.18	0.17	0.6%	± 0.013
Groundgear 3	5	0.26	0.25	1.4%	± 1.463
	10	0.20	0.18	2.1%	± 0.597
Groundgear 4	1	0.45	0.37	8.3%	± 0.093
	12	0.20	0.13	7.2%	± 0.271
Groundgear 5	4	0.25	0.18	6.8%	± 0.477
	13	0.18	0.14	4.4%	± 0.301
Groundgear 6	3	0.44	0.52	-8.0%	± 0.404
	9	0.15	0.18	-3.8%	± 2.585

Table 7. Predicted percentage of downed sea whips in impact and control areas by experimental gear and track.

		Downed Sea Whips			
Experimental Gear ID	Track	Impact	Control	% Difference	95% CI
Groundgear 1	7	14.9%	9.8%	5.1%	± 2.4%
	11	15.4%	12.7%	2.7%	± 1.9%
Groundgear 2	8	18.6%	15.0%	3.5%	± 1.8%
	14	22.4%	6.3%	16.1%	± 3.6%
Groundgear 3	5	13.9%	10.1%	3.8%	± 2%
	10	24.0%	11.3%	12.7%	± 3%
Groundgear 4	1	18.3%	9.3%	8.9%	± 3.6%
	12	16.6%	11.0%	5.5%	± 2.4%
Groundgear 5	4	20.6%	10.3%	10.3%	± 3%
	13	19.1%	8.9%	10.2%	± 3%
Groundgear 6	3	12.2%	7.8%	4.4%	± 2.2%
	9	13.1%	10.7%	2.4%	± 2.4%

Table 8. Nominal (A) and susceptibility-adjusted swept area (A_s) by experimental gear and track.

Experimental Gear ID	Track	Nominal Swept Area (km^2)	Susceptibility-Adjusted Swept Area (km^2)	Ratio A_s/A
Groundgear 1	7	0.337	0.017	5.1%
	11	0.337	0.009	2.7%
Groundgear 2	8	0.308	0.011	3.5%
	14	0.324	0.052	16.1%
Groundgear 3	5	0.354	0.014	3.8%
	10	0.297	0.038	12.7%
Groundgear 4	1	0.273	0.024	8.9%
	12	0.333	0.018	5.5%
Groundgear 5	4	0.331	0.034	10.3%
	13	0.320	0.032	10.2%
Groundgear 6	3	0.313	0.014	4.4%
	9	0.420	0.010	2.4%

Table 9. Predicted percentages of damaged sea whips in impact and control areas by experimental gear and track.

Experimental Gear ID	Track	Impact	Control	% Difference	95% CI
		Damaged Sea Whips			
Groundgear 1	7	2.9%	0.6%	2.3%	± 3%
	11	3.9%	1.7%	2.2%	± 3.2%
Groundgear 2	8	1.4%	0.4%	1.0%	± 2.1%
	14	5.2%	1.2%	4.0%	± 3.9%
Groundgear 3	5	4.5%	0.4%	4.1%	± 4%
	10	3.4%	2.3%	1.1%	± 2.9%
Groundgear 4	1	1.1%	0.4%	0.7%	± 1.4%
	12	3.7%	1.5%	2.2%	± 3.2%
Groundgear 5	4	1.4%	0.3%	1.0%	± 1.9%
	13	2.7%	0.6%	2.1%	± 2.9%
Groundgear 6	3	0.6%	0.0%	0.6%	± 1.3%
	9	2.0%	1.4%	0.7%	± 2.6%

FIGURES

Figure 1. Study location (white dot) in the Eastern Bering Sea, southeast of the Pribilof Islands.

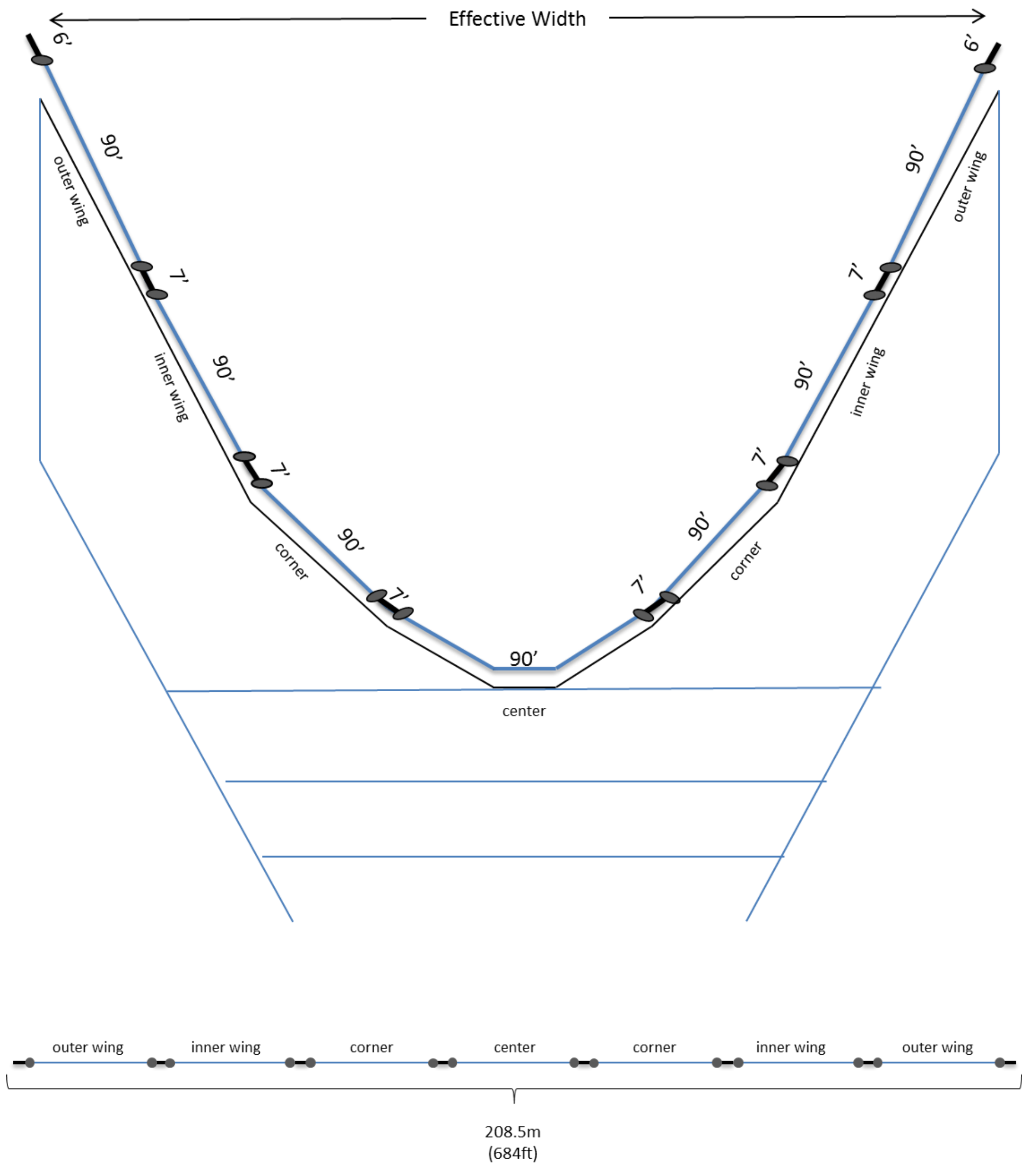

Figure 2. Schematic of the raised footrope configuration with 27.4 m (90 ft) material sections and 2.1 m (7 ft) weight chain, bobbin sections, and the effective width. The material sections are labeled as outer wing, inner wing, corner and center.

Figure 3. Weight chain 2.1 m (7 ft) with a steel bobbin 25.4 cm (10 in diameter) on each end.

Figure 4. Spectra loop (1.2 m (4 ft); when attached creates a 0.6 m (2 ft) spacing) that replaced the conventional 1 m dropper chain.

Figure 5. Three rope types: ¾ in Spectra, 2 in combination wire (combi), 2 in polyethylene rope (poly).

Groundgear 1 *(all poly no bobbins)*

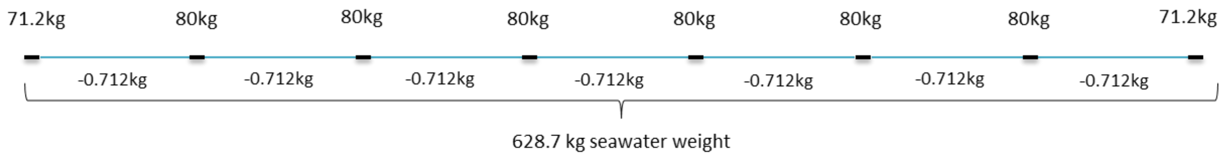

Groundgear 2 *(Spectra-combi-combi30-poly)*

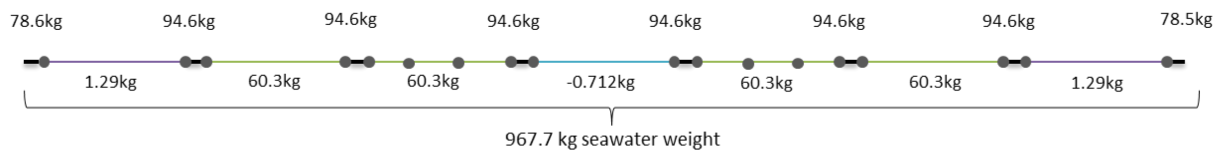

Groundgear 3 *(combi-combi30-poly-Spectra)*

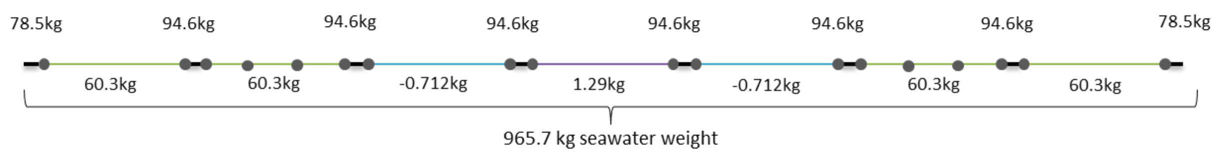

Groundgear 4 *(combi30-poly-Spectra-combi45)*

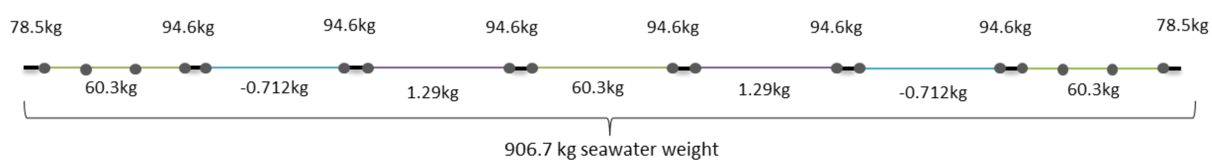

Groundgear 5 *(poly-Spectra-combi-combi45)*

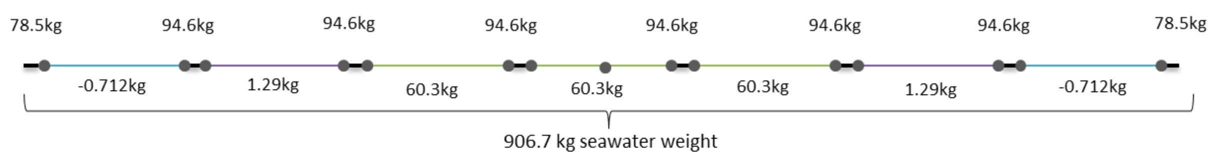

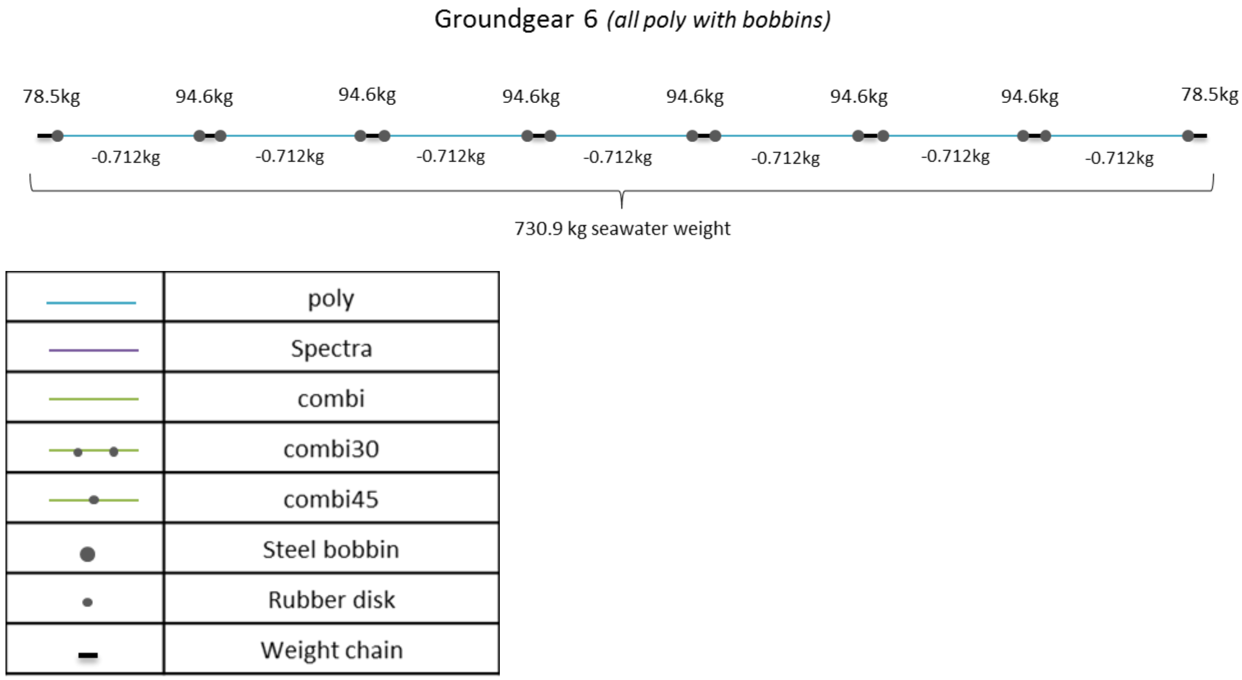

Figure 6. Each raised footrope configuration labeled Groundgear 1-6 with the specific seawater weight of each component and entire footrope.

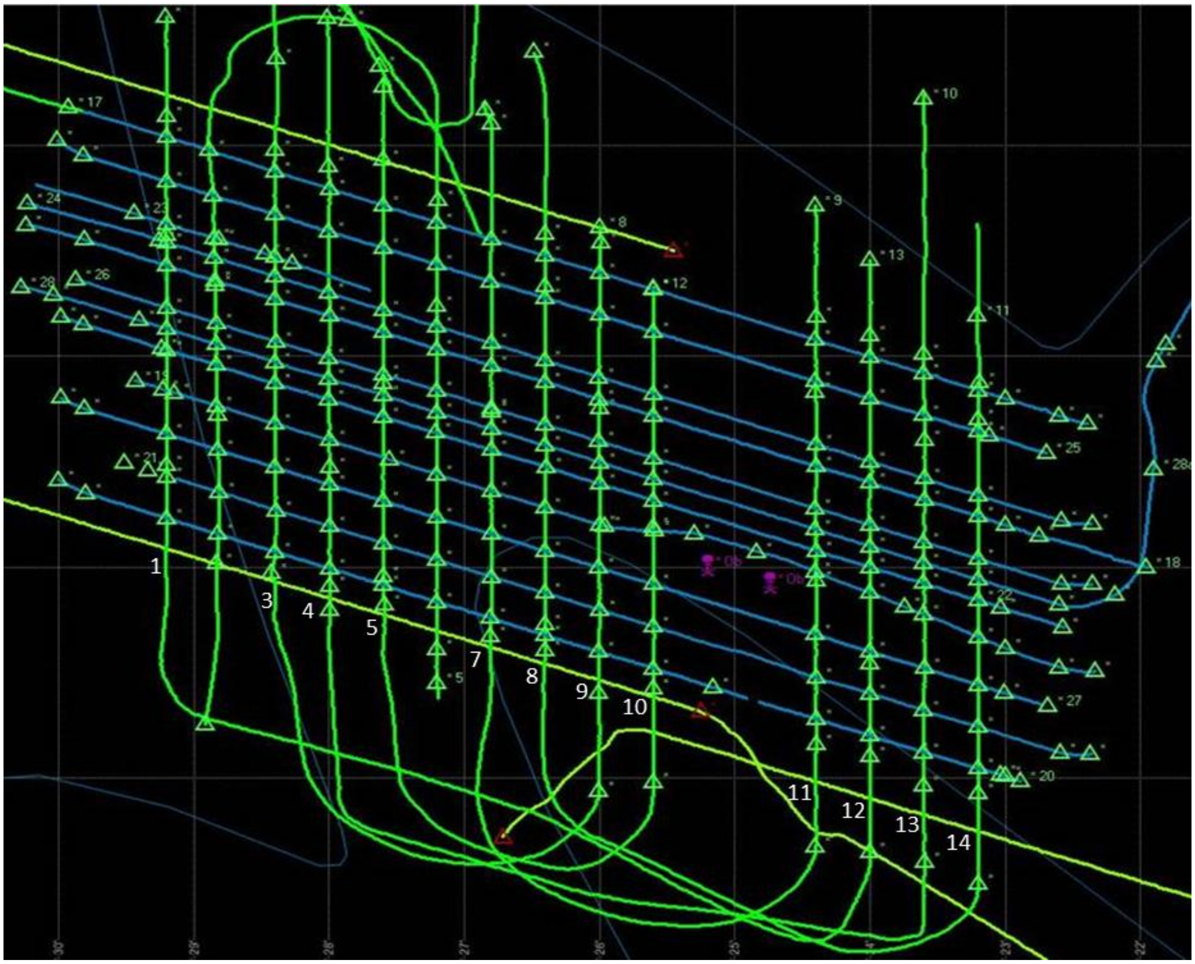

Figure 7. Six groundgear configurations towed twice, north to south and south to north, are shown in green. Note the two additional lines were test tows conducted with a bottom trawl (between 1 and 3, and 5 and 7). The ten acoustic/ video transects crossing perpendicular to the trawl tows are shown in blue. The black areas between the green trawl lines are the control areas. Note: the triangles are not an indicator direction.

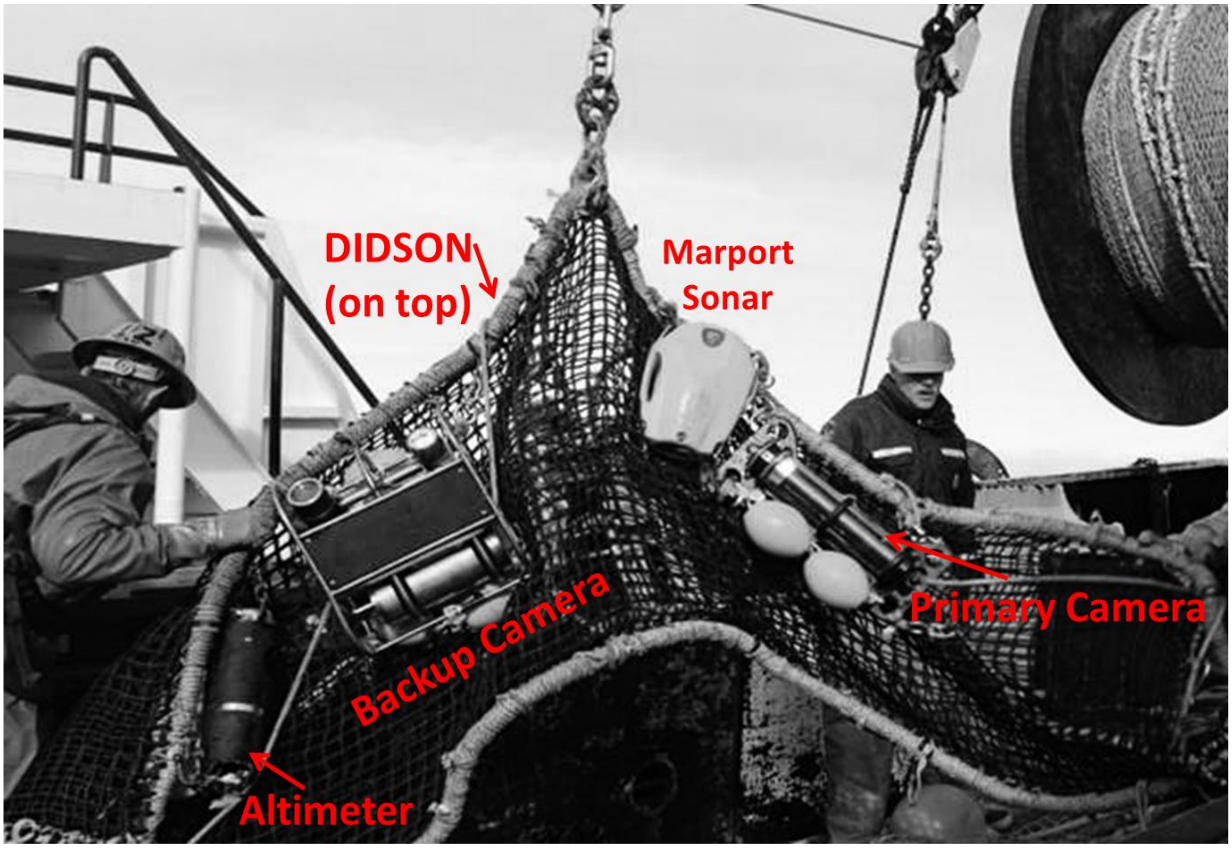

Figure 8. The mesh panel that attaches to the bottom trawl during observation tows has five observation units attached to it. Altimeter: bottom starboard. Backup camera: bottom starboard. Marport Sonar: bottom port. Primary camera: bottom port. DIDSON: top center (not visible in photo).

Figure 9. The DIDSON unit is housed inside protective cage with floats and attached to the top center of the mesh panel.

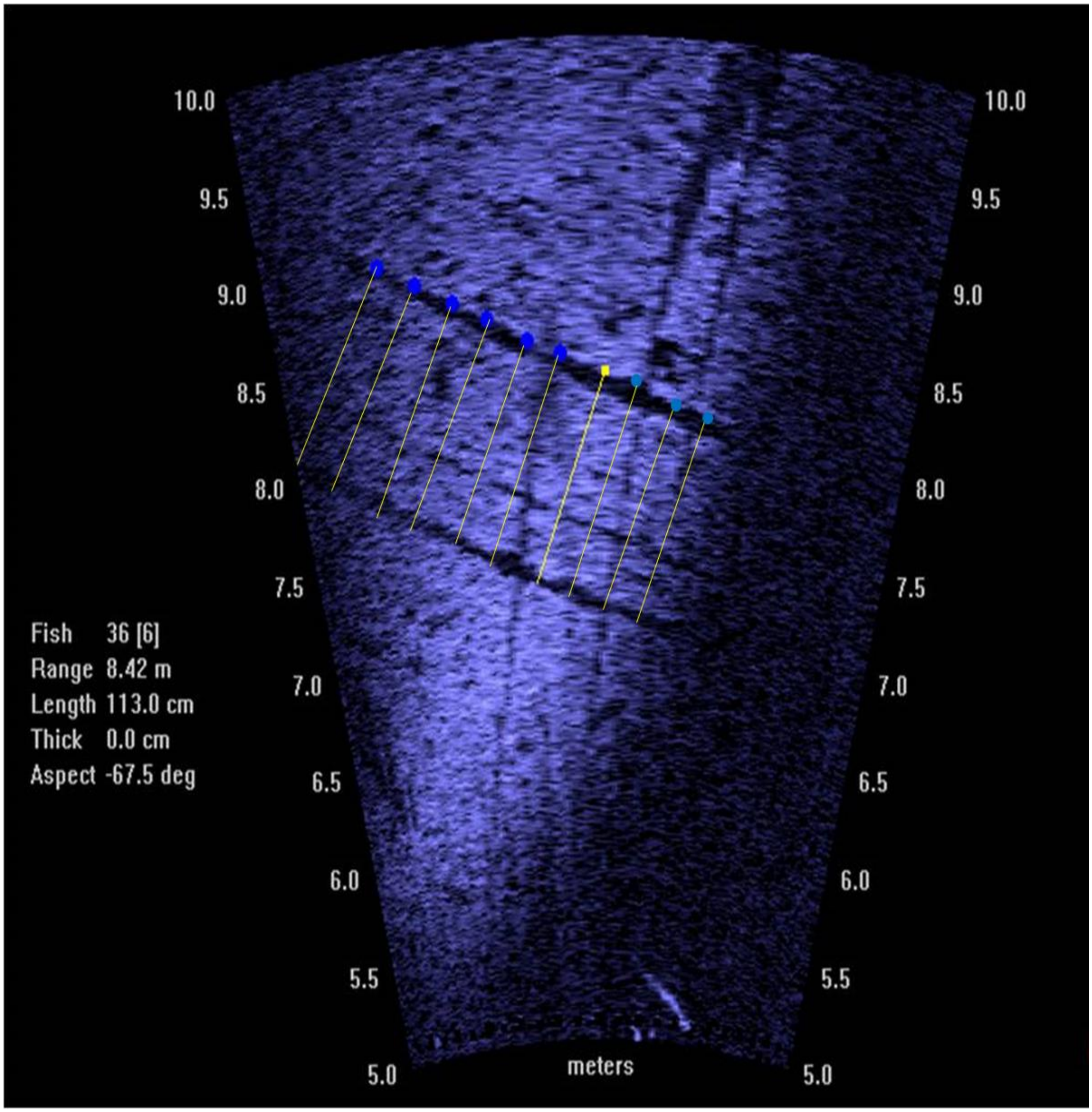

Figure 10. The DIDSON imagery used to identify and measure scours in the seafloor. The yellow lines represent the ten widths measured for each mark within the track.

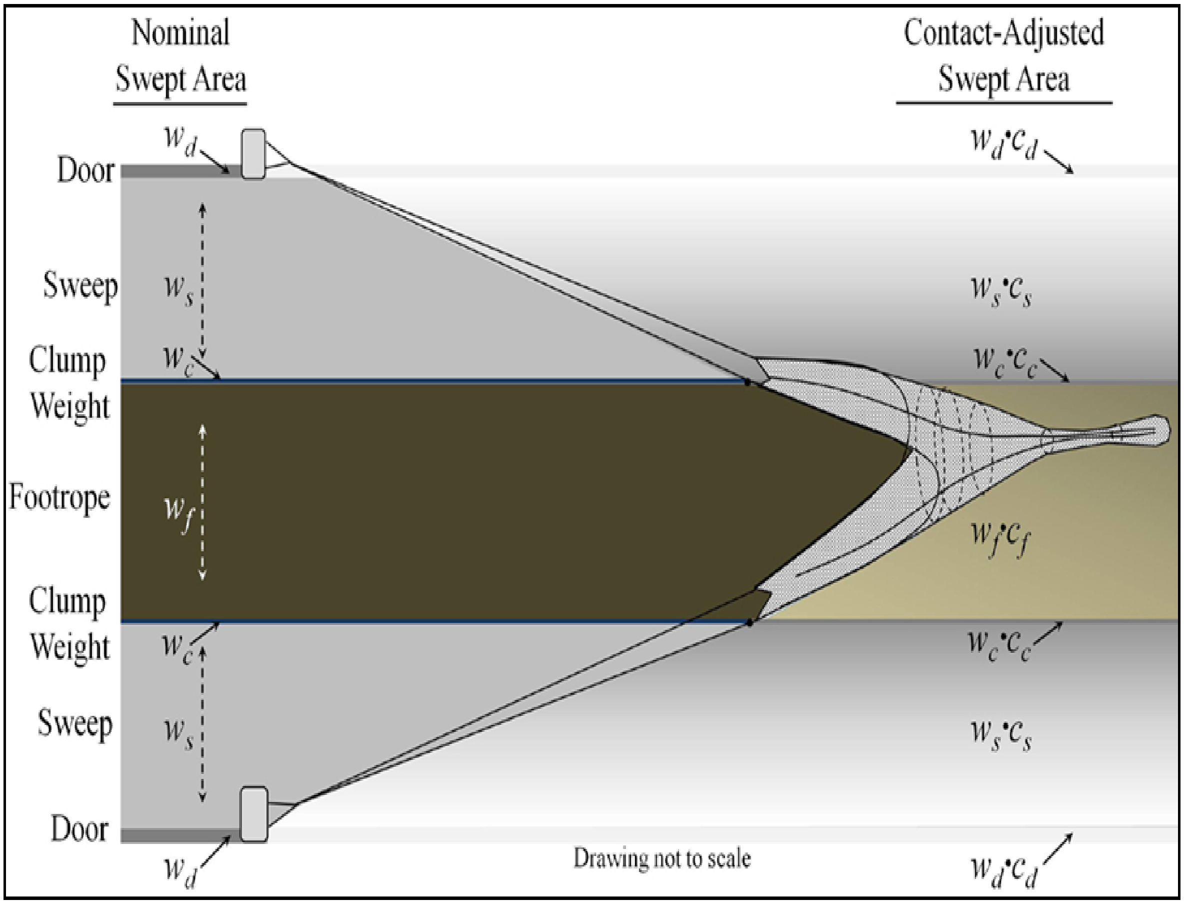

Figure 11. Diagram of a stylized trawl demonstrating nominal and contact-adjusted swept area by door, sweep, and footrope. The nominal swept area is the potential contact of each component i.e., w_d = effective width of a door, w_c = effective width of a clump weight (m), w_s = effective width of a sweep (m), which equals sweep length·sin (α_s), where α_s = sweep angle, w_{fw} = effective width of a footrope wing (m), which equals to the spread of the lower wing, and w_{fc} = effective width of the footrope center (m). The contact-adjusted swept area uses actual contact as component-specific modifiers ("contact indicies") to weight the proportion of contact i.e., c_d = contact index, door, c_c = contact index, clump weight, c_s = contact index, sweeps, c_{fw} = contact index, footrope wing, and c_{fc} = contact index, footrope center.

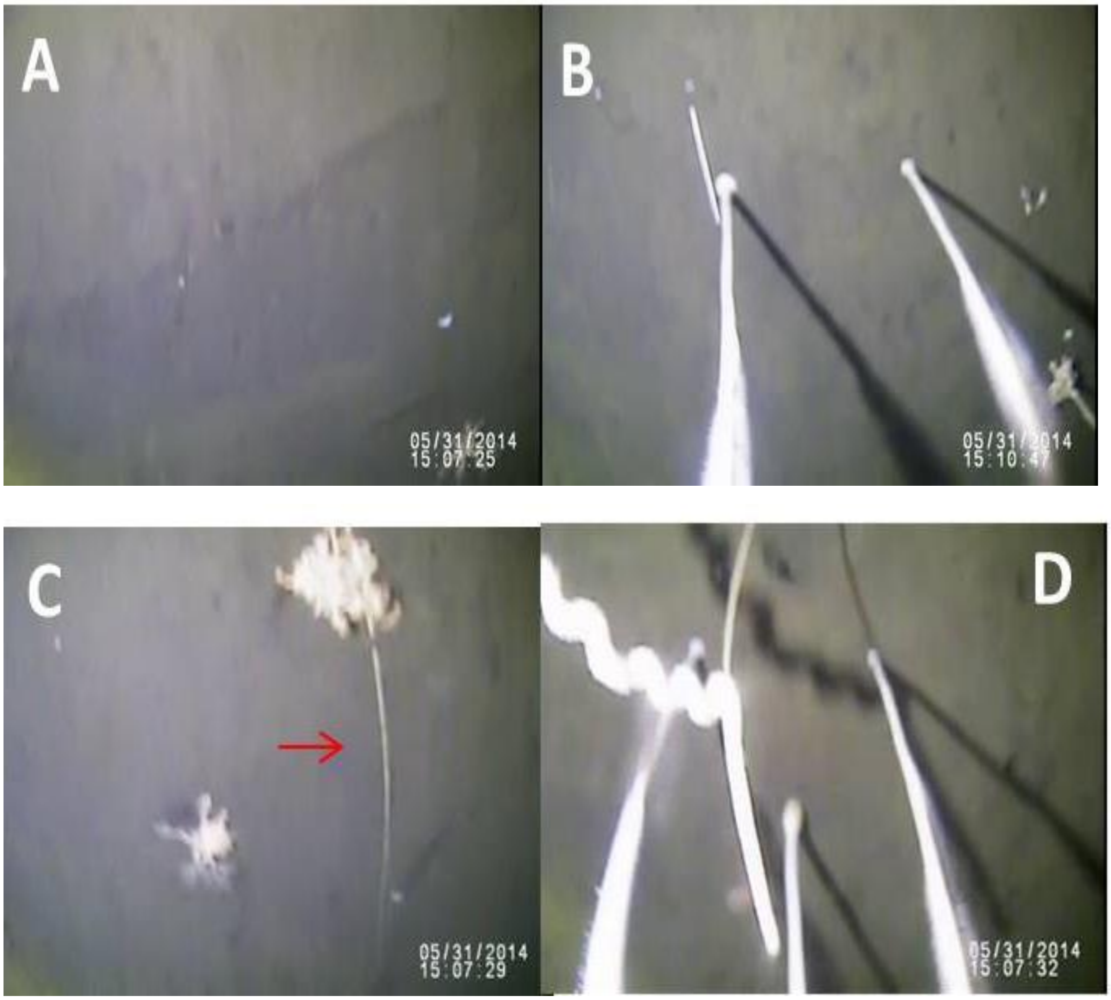

Figure 12. Primary camera imagery of A) a scour in the seafloor; B) up/intact sea whips; C) downed/dislodged sea whip; and D) damaged sea whip with flesh stripped off.

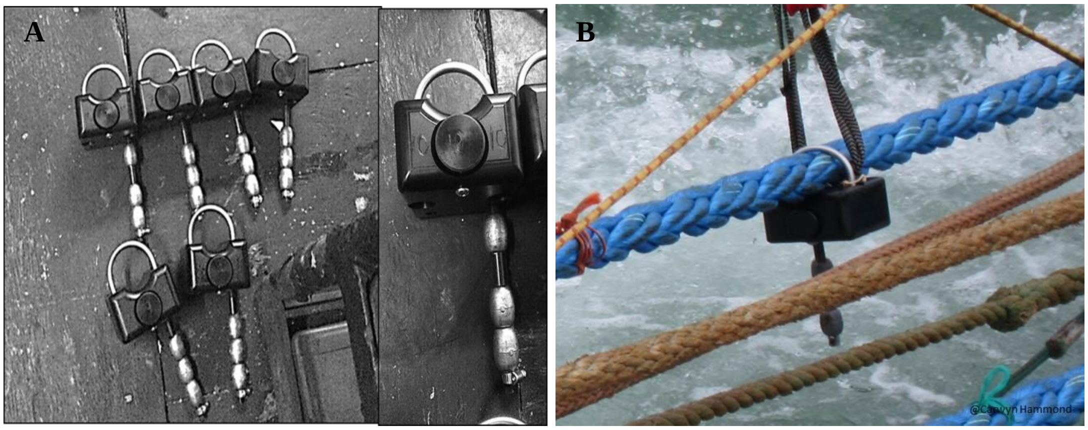

Figure 13. Bottom contact sensor housing units, labeled for placement on the footrope (A) and attached to the rope mid-span (B).

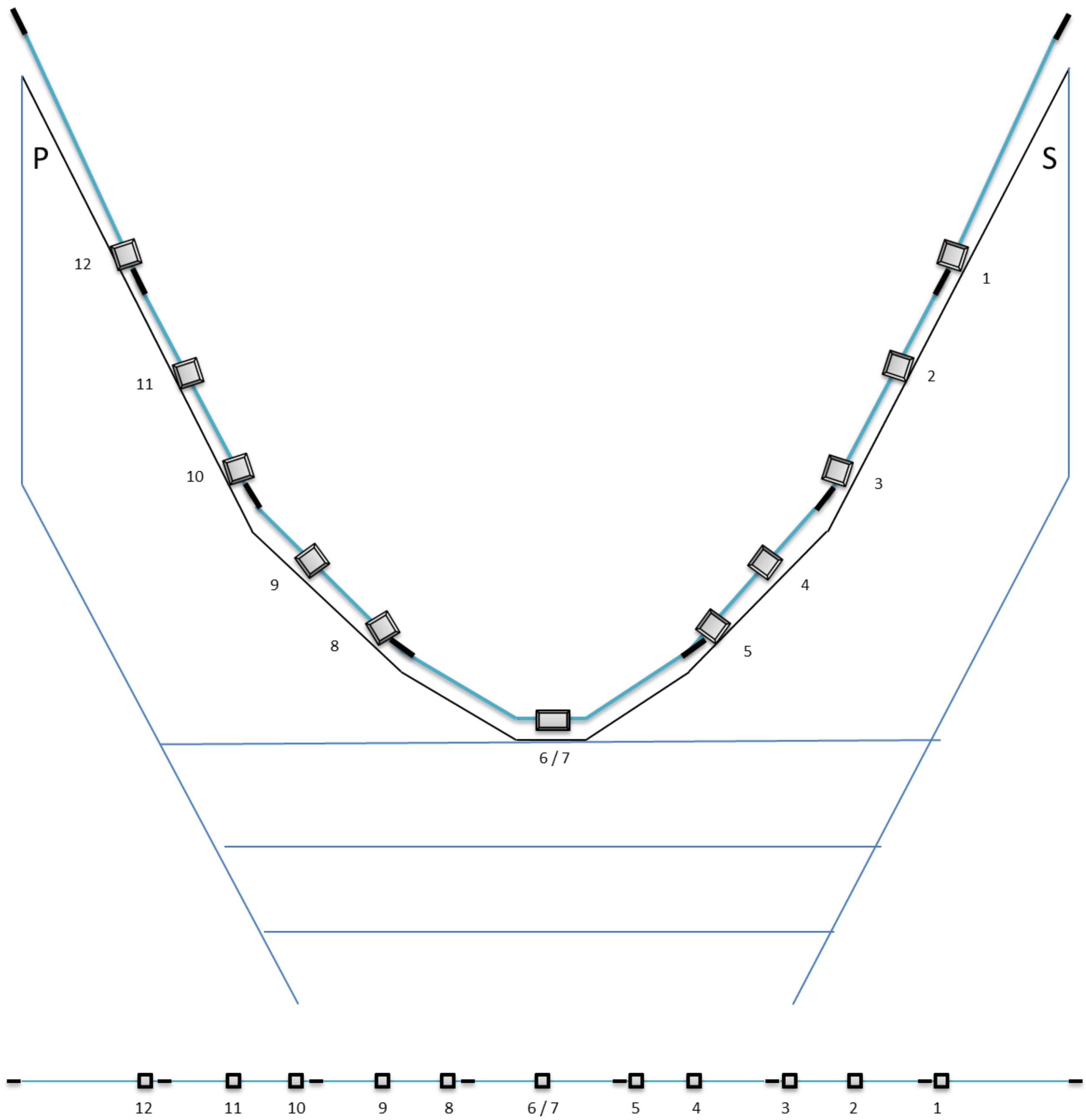

Figure 14. Placement locations of the 12 bottom contact sensors on the groundgear during experimental tows. Bottom contact sensors are labeled 1-12 from starboard to port respectively.

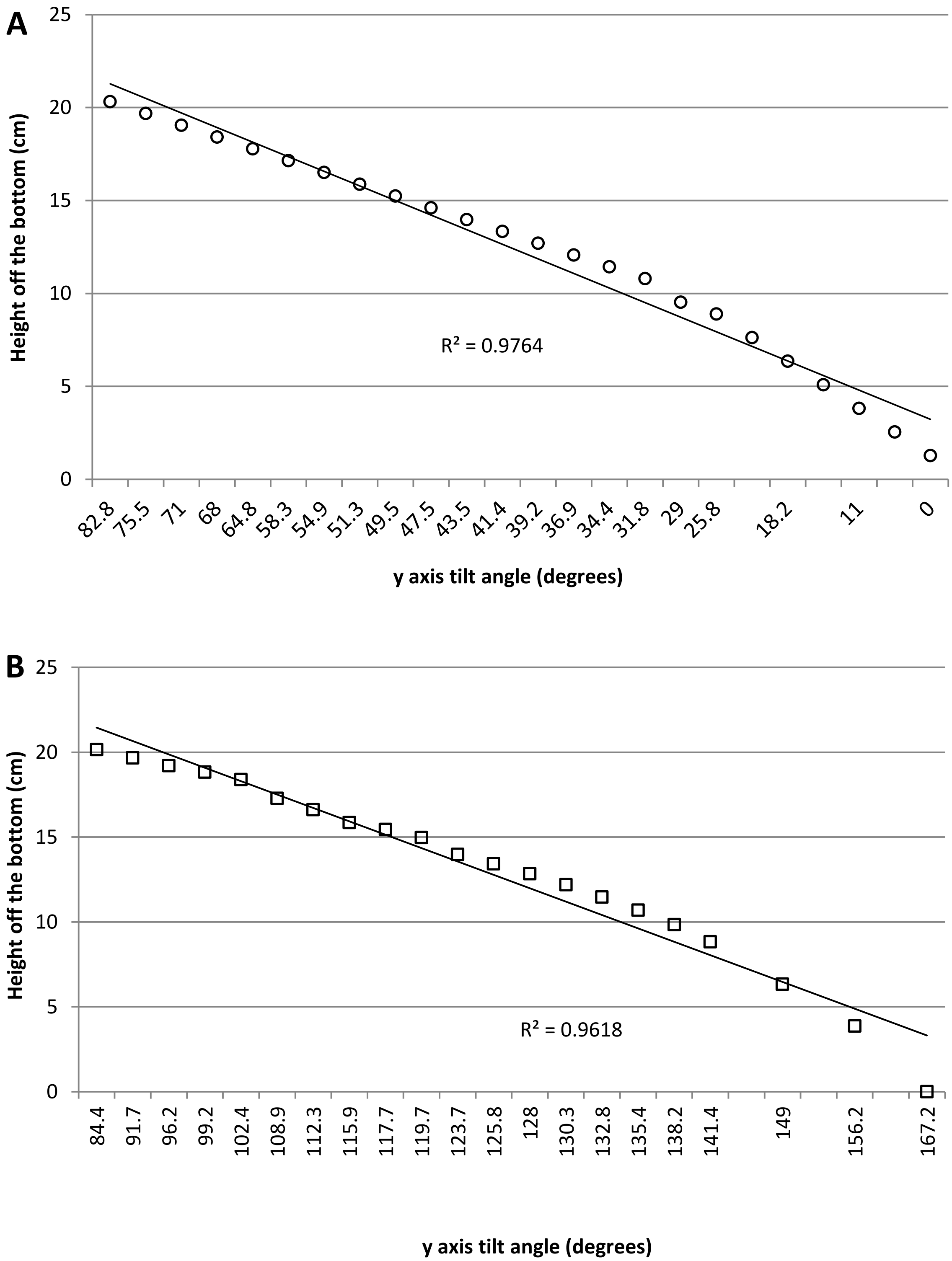

Figure 15. Tilt sensor calibration curve describing the relationship between the y angle measured by the accelerometer and the measured height off the bottom for A) starboard attachments, and B) port attachments.

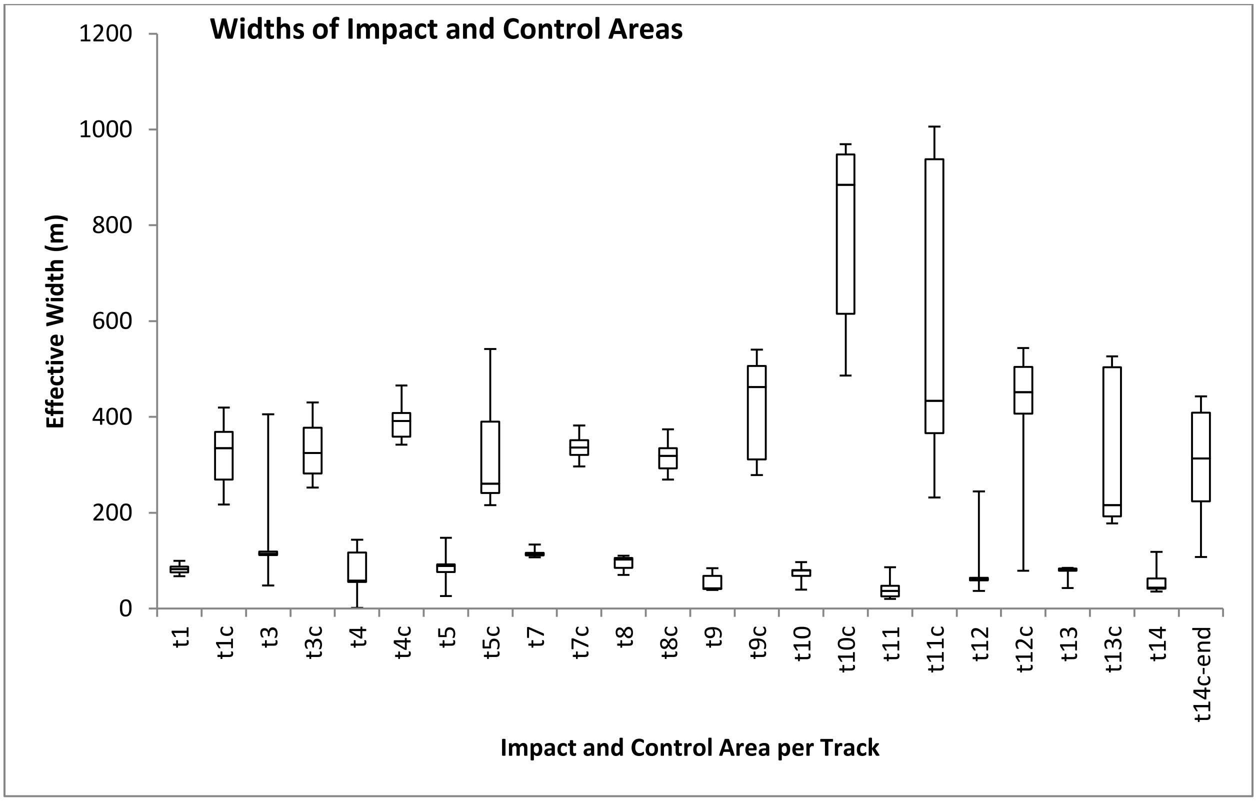

Figure 16. Effective widths (see Figure 2) of the impact and adjacent control area measured from observation transects (DIDSON and video). On the x-axis, t=track and c=control. Note: the large control winds for tracks 10 and 11 are due to obstruction avoidance (see figure 7).

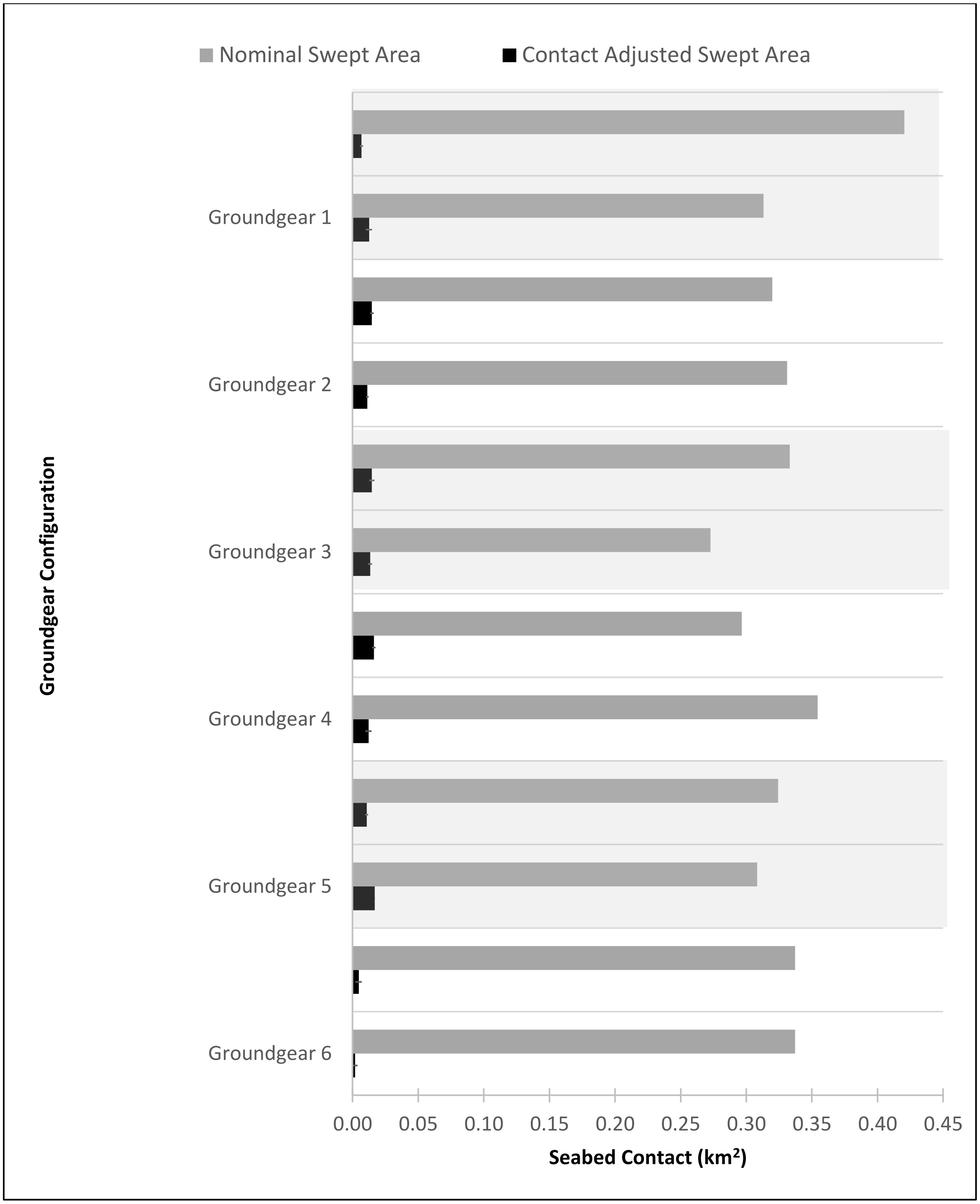

Figure 17. The nominal (A) and contact-adjusted (A_c) swept area estimates in square kilometers for each footrope configuration. Nominal swept area is depicted by grey bars and the corresponding contact-adjusted swept area is depicted by black bars and the 95% confidence intervals.

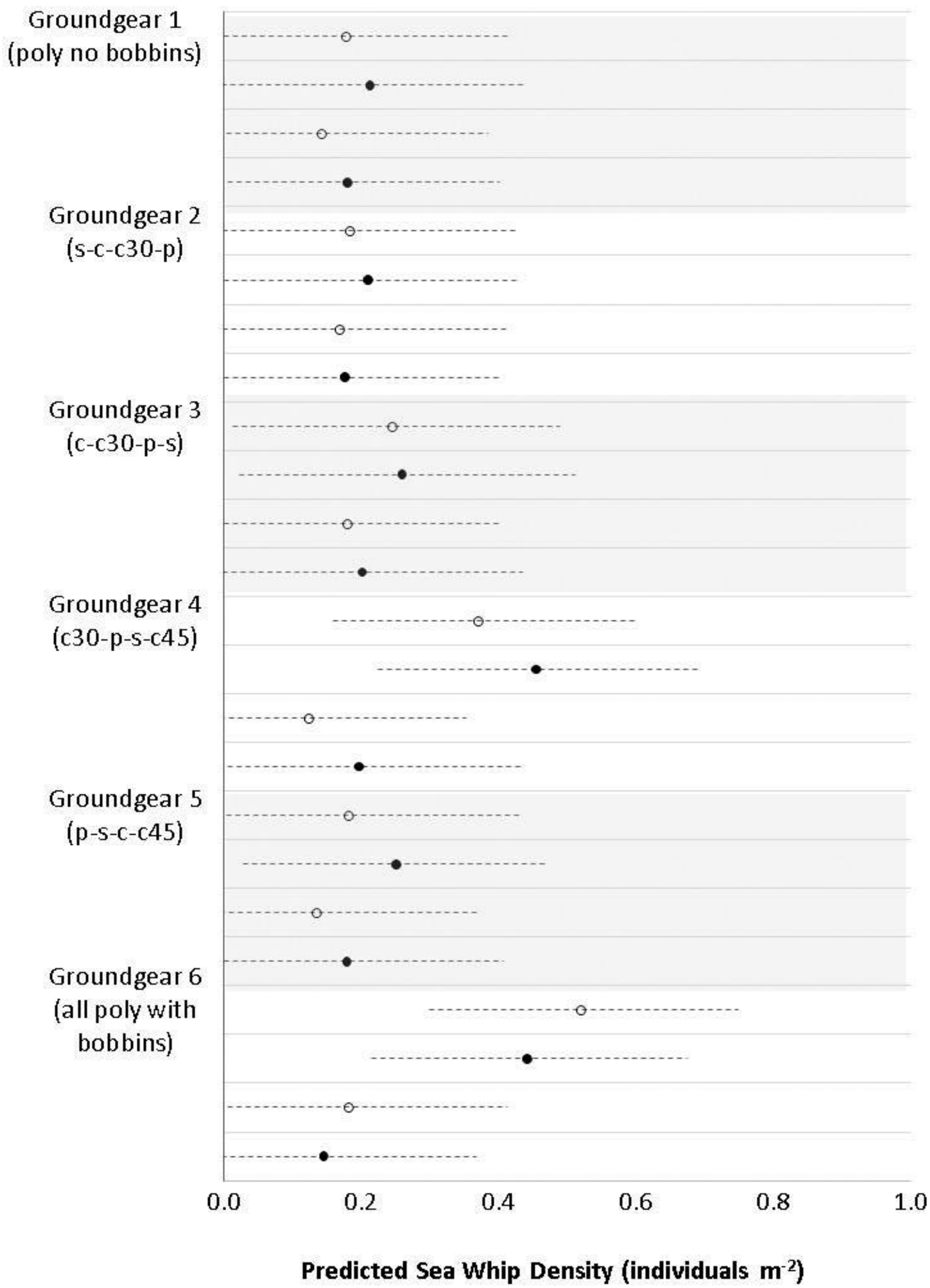

Figure 18. Comparability of control and impact areas is described by the likeness of sea whip densities (individuals per m^{-2}) for each track and the 95% confidence intervals. The solid black dots indicate data from the impact area and the white dots are from the control area.

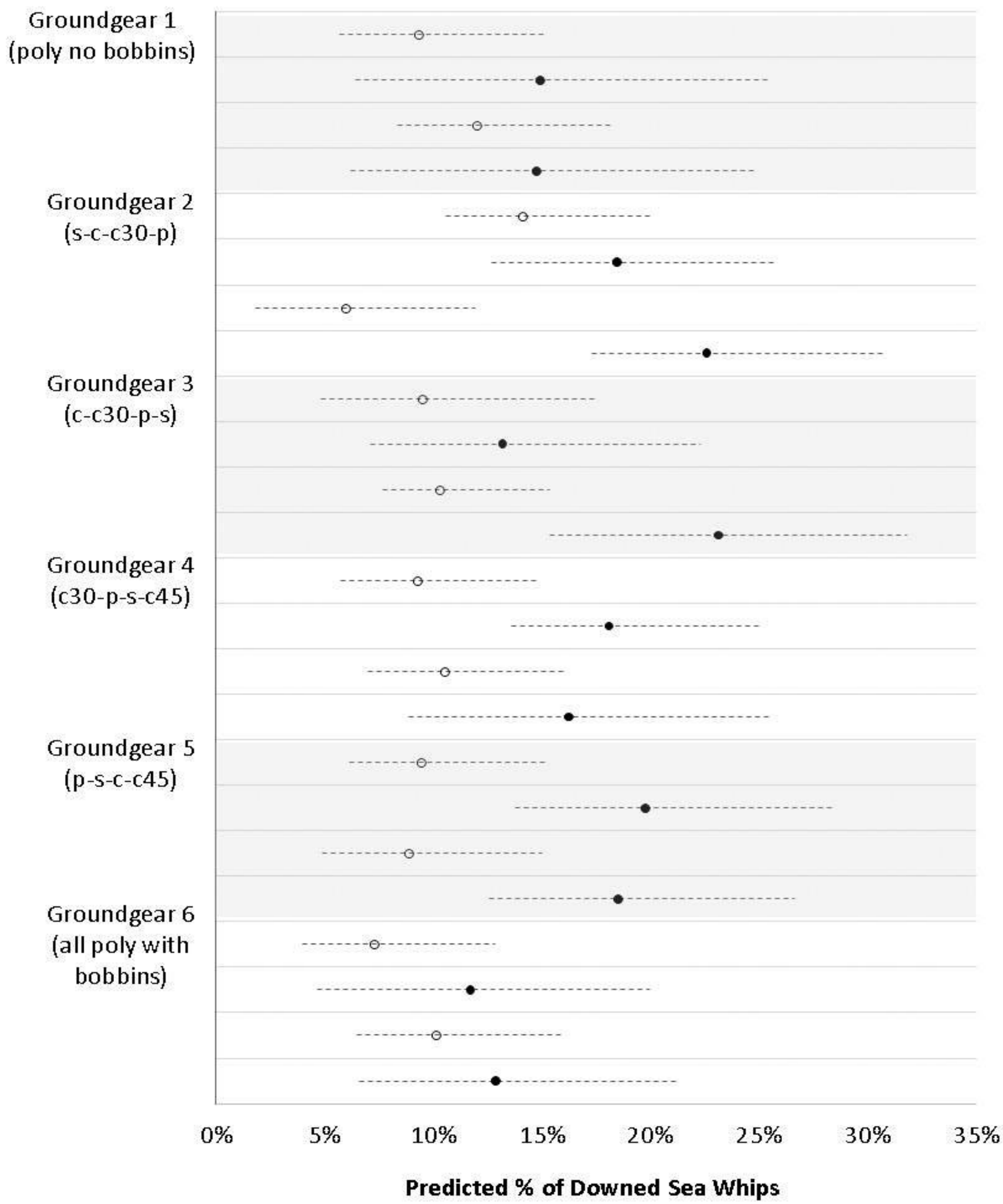

Figure 19. Susceptibility indices are described by the predicted percent of downed sea whips in the impact and adjacent control area of each trawl and the 95% confidence intervals. The solid black dots indicate data from the impact area and the white dots are from the control.

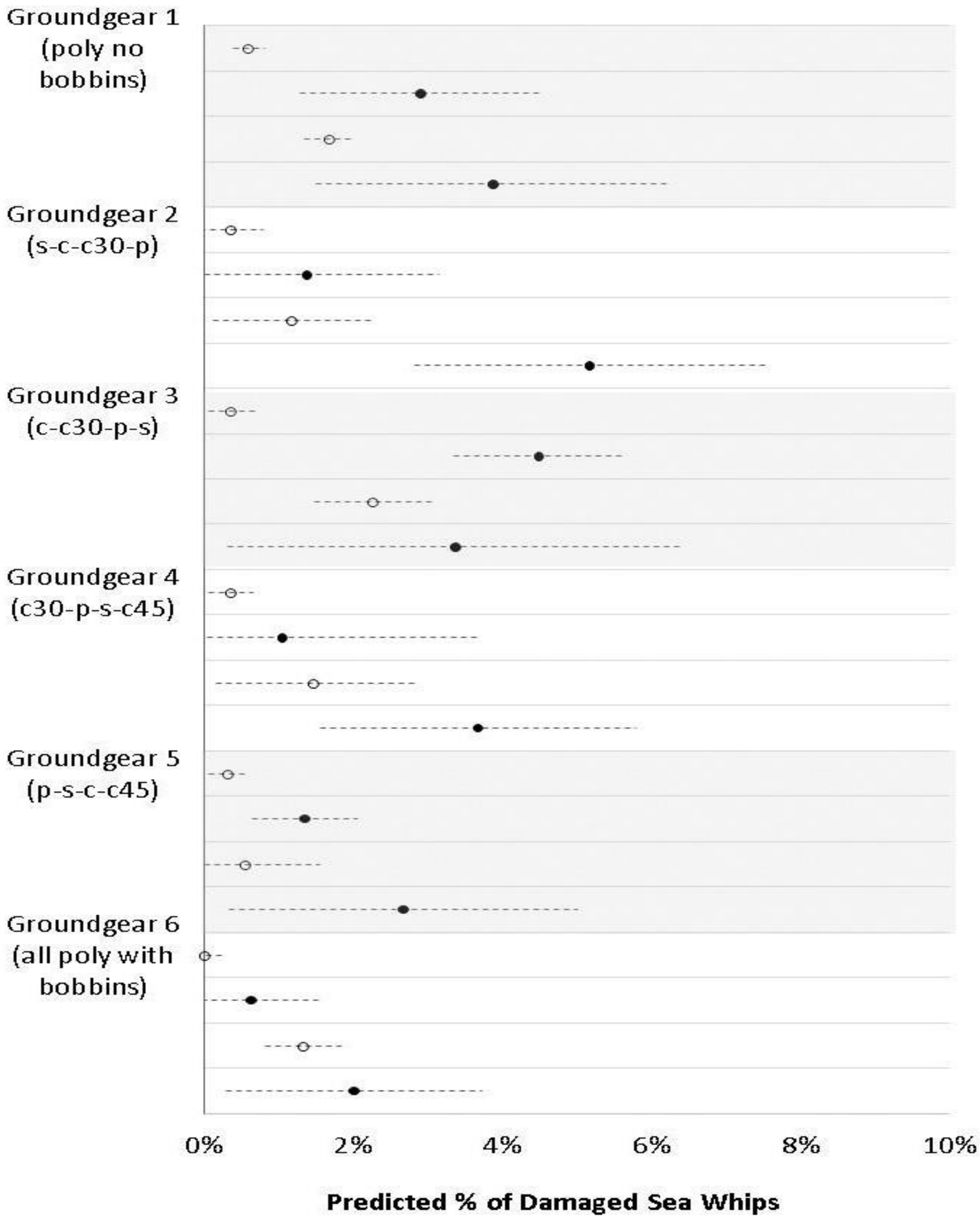

Figure 20. Predicted percent of damaged sea whips in the impact and adjacent control area of each trawl and the 95% confidence intervals. The solid black dots indicate data from the impact area and the while dots are from the control.

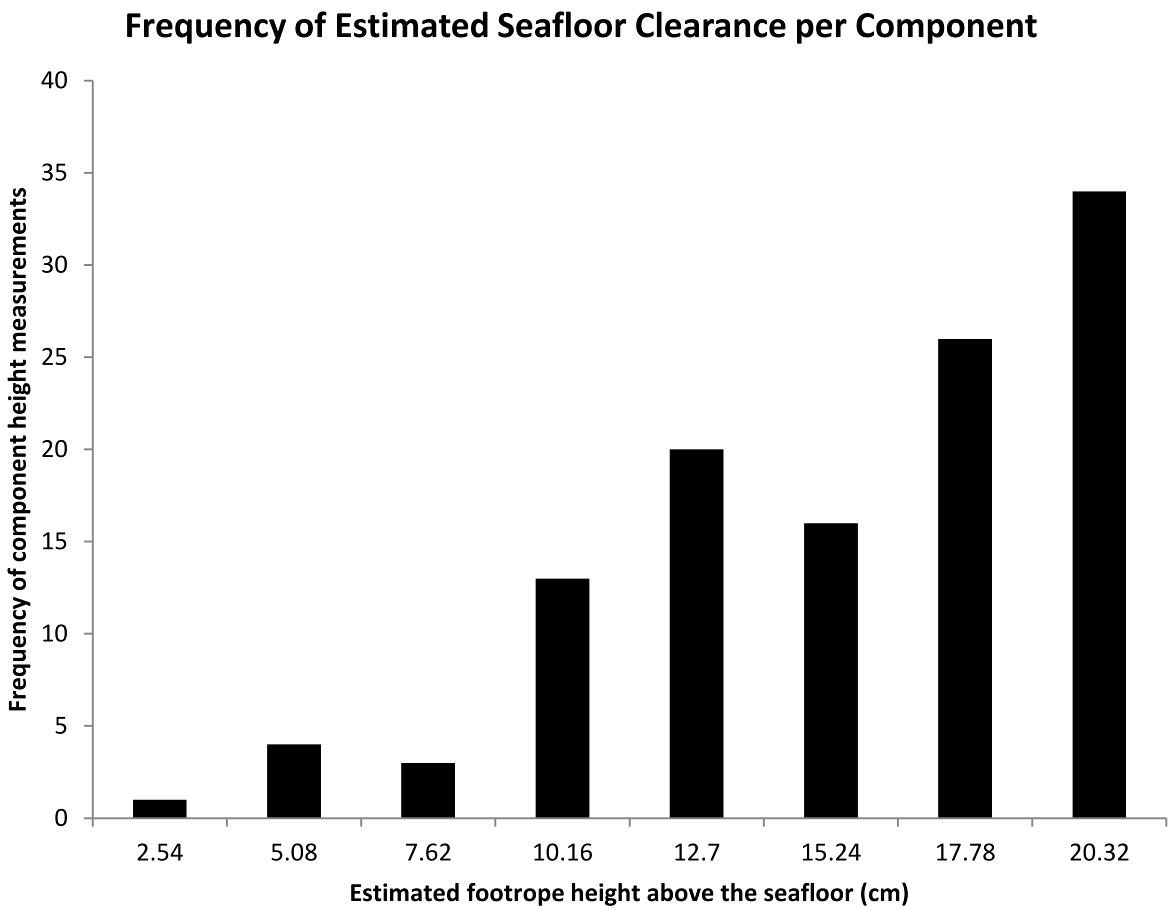

Figure 21. The frequency of mean clearance heights from all 12 sensors during each experimental tow are displayed in the histogram. The bins range from 2.54 cm (1 in) to 20.32 cm (8 in).

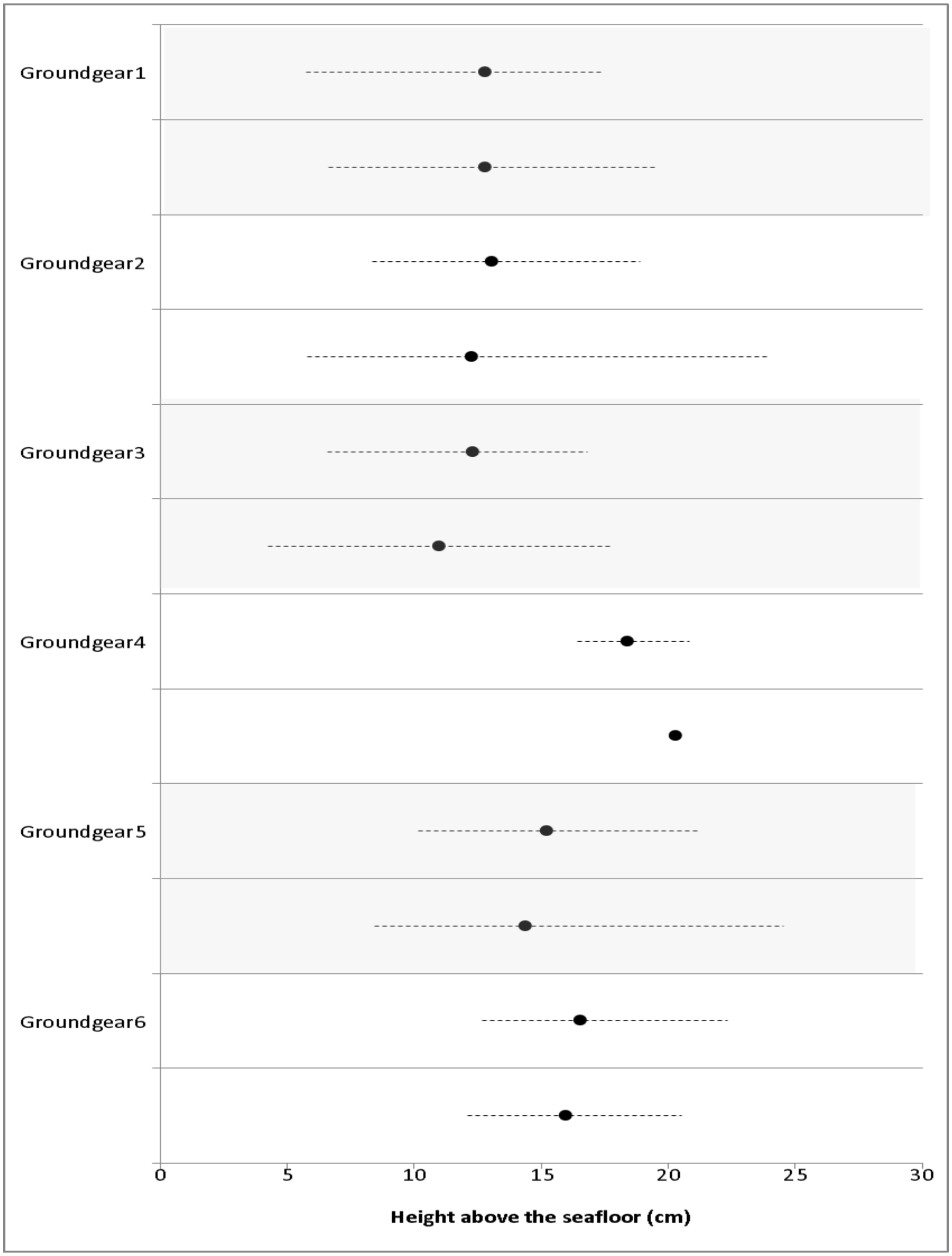

Figure 22. The average height above the seafloor for each track is displayed in centimeters with the variation described by maximum and minimum values.

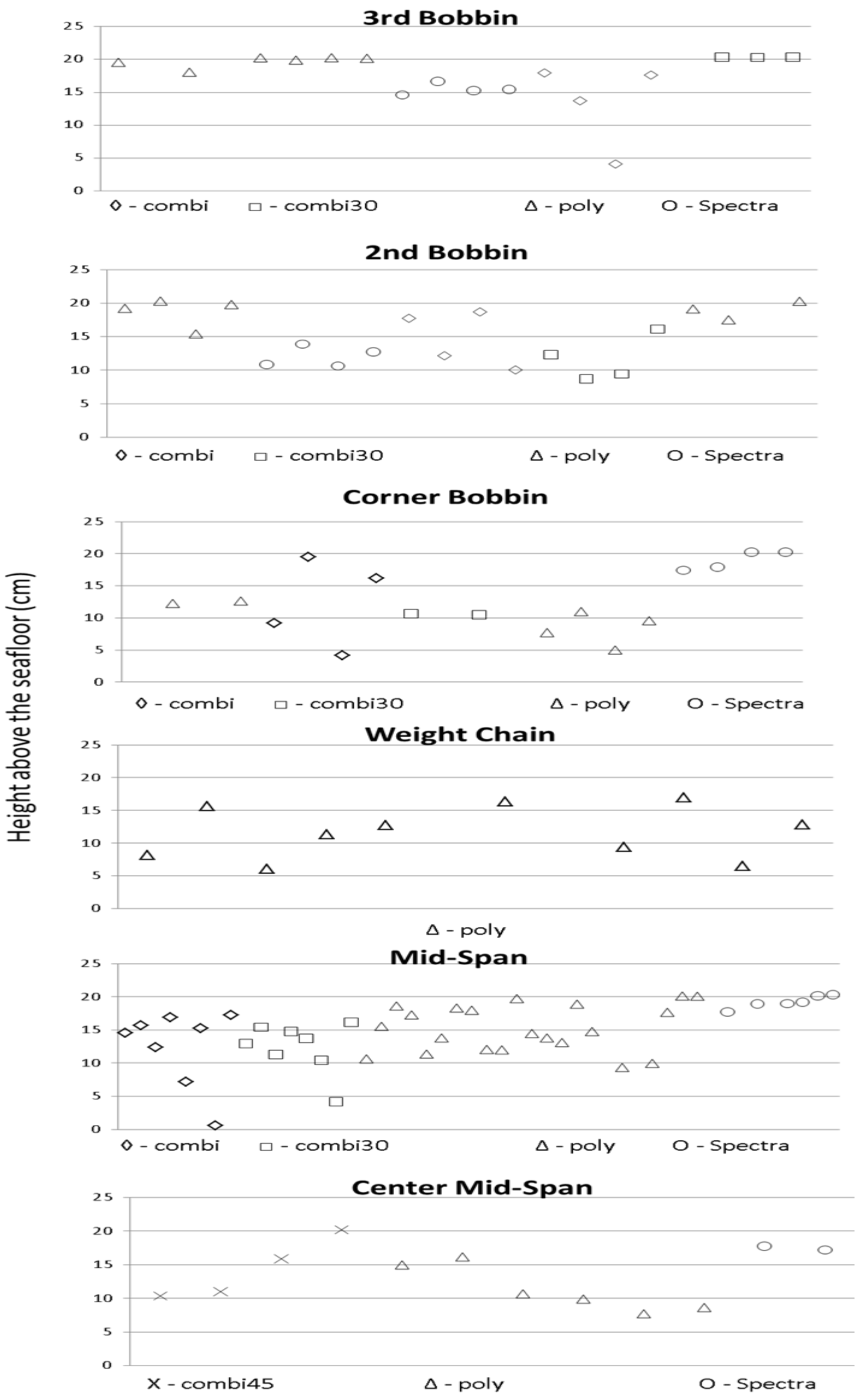

Figure 23. Seafloor clearance estimates for each location and material type, describing the effect of the interactions on seafloor clearance. Each plot describes the interaction of location and material types have on the seafloor clearance. Diamonds represent poly, squares represent combi30, ‘X’ represent combi45, circles represent Spectra, and triangles represent poly.

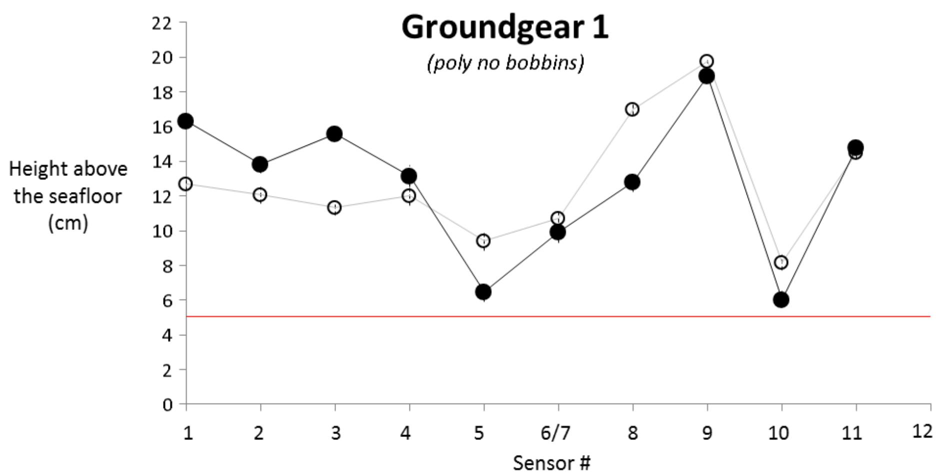
Groundgear 1
(poly no bobbins)
Height above the seafloor (cm)
22
20
18
16
14
12
10
8
6
4
2
0
1
2
3
4
5
6/7
8
9
10
11
12
Sensor #

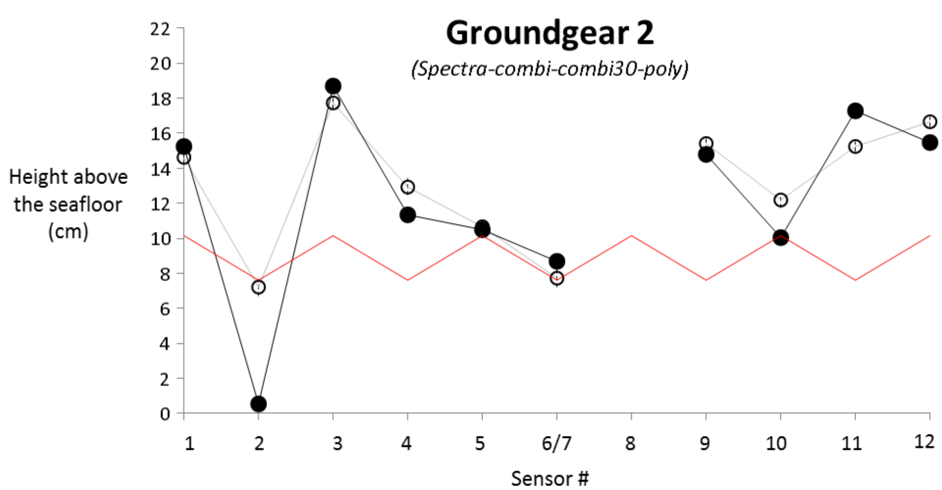
Groundgear 2
(Spectra-combi-combi30-poly)
Height above the seafloor (cm)
22
20
18
16
14
12
10
8
6
4
2
0
1
2
3
4
5
6/7
8
9
10
11
12
Sensor #

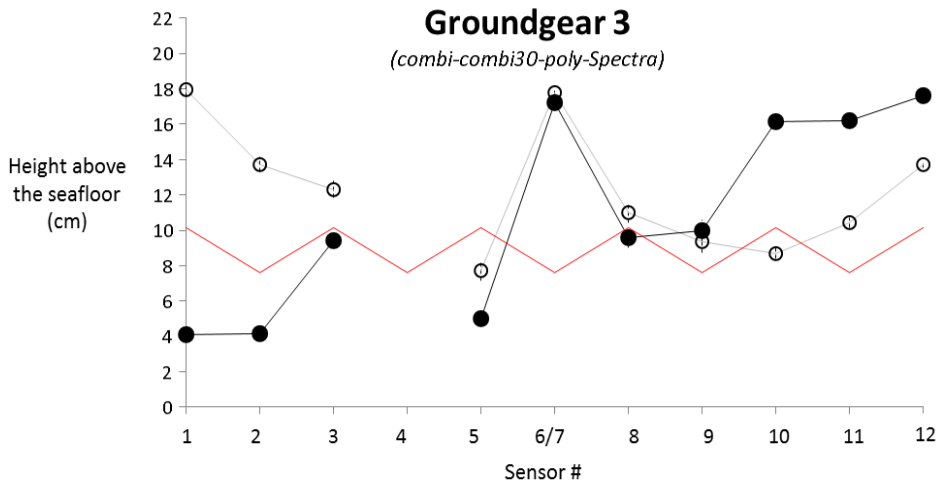
Groundgear 3
(combi-combi30-poly-Spectra)
Height above the seafloor (cm)
Sensor #
0
2
4
6
8
10
12
14
16
18
20
22
1
2
3
4
5
6/7
8
9
10
11
12

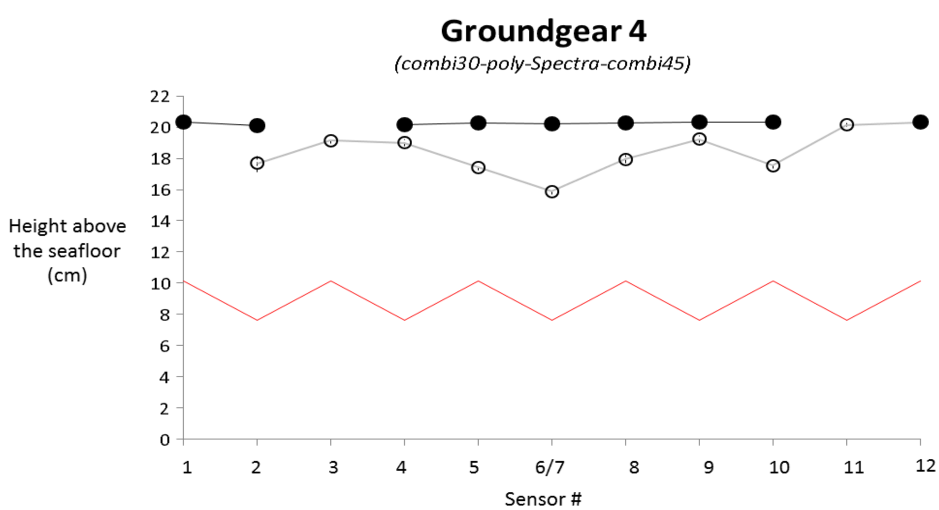
Groundgear 4
(combi30-poly-Spectra-combi45)
Height above the seafloor (cm)
Sensor #
0
2
4
6
8
10
12
14
16
18
20
22
1
2
3
4
5
6/7
8
9
10
11
12

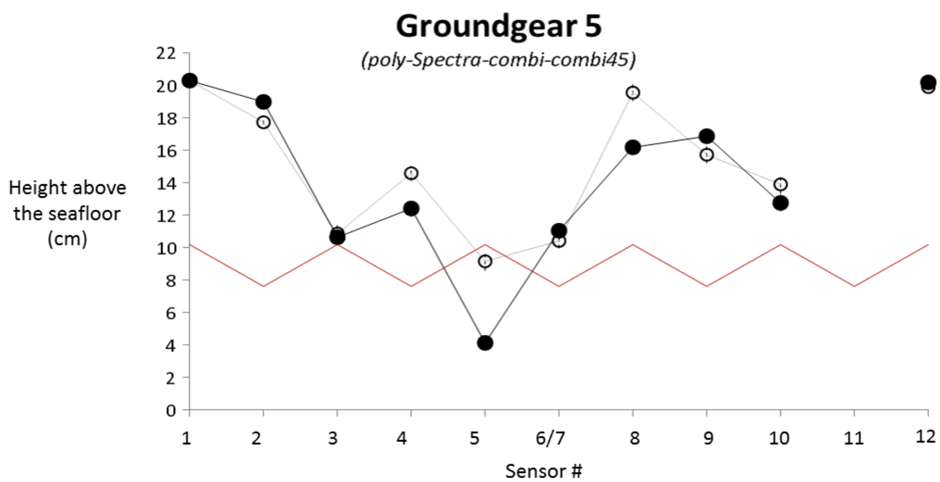

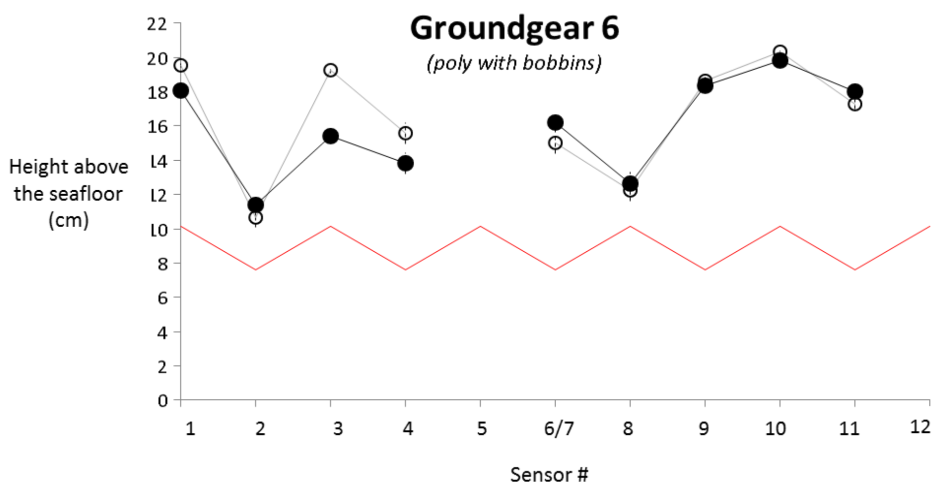

Figure 24. Average seafloor clearance estimates of each component per track are plotted for each raised footrope configuration (Groundgear1-6). Described are the configuration's effect on seafloor clearance and the change in clearance as the material types are alternated through the locations of the configuration. The red line depicts the least expected height of each component.

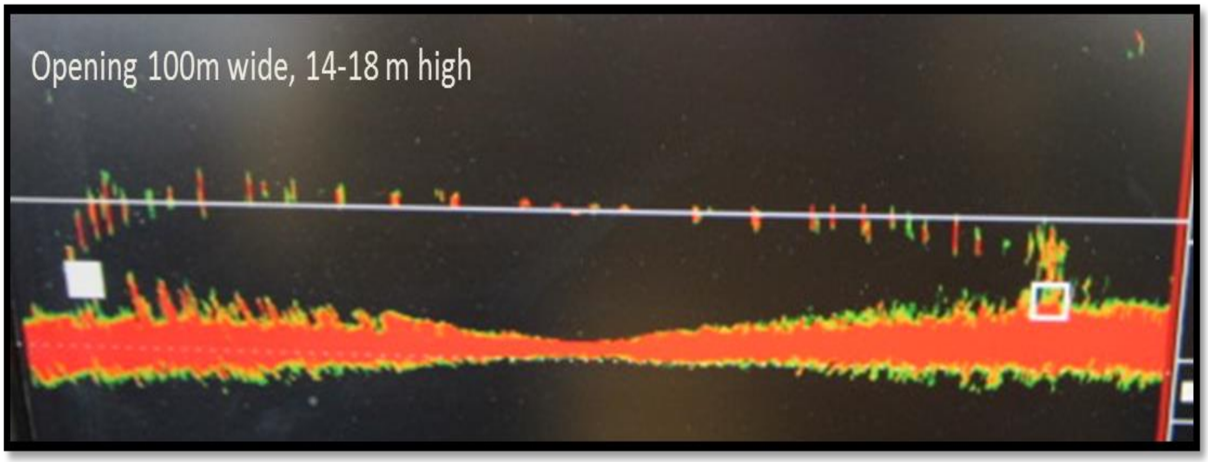

Figure 25. The net mensuration (Wesmar 770) display showing no apparent bottom separation of raised footrope on the pelagic trawl during fishing practicality test. The white boxes indicate the wing tips. The opening measurements are the width (100 m) from wing tip to wing tip and height (14-18 m) from the footrope to the headrope.

APPENDIX

Table A.1. Trace plots for parameters estimated by the Bayesian GLMM that include sea whip distribution within impact and control areas.

#model notation <- MCMCglmm(SW.All.dens ~ Reserve + Haul + Reserve:Haul, random = ~Track,data=my.dat,family="gaussian", verbose=F, nitt=25000, burnin=20000, thin=5, pr=T)

Summary of MCMCglmm

Iterations = 20001:24996 Thinning interval = 5 Sample size = 1000

DIC: 189.7235

G-structure: ~Track

	post.mean	l-95% CI	u-95% CI	eff.samp
Track	0.03702	0.005291	0.08547	1114

R-structure: ~units

	post.mean	l-95% CI	u-95% CI	eff.samp
units	0.1024	0.08219	0.1183	754.1

Location effects: SW.All.dens ~ Reserve + Haul + Reserve:Haul

	post.mean	l-95% CI	u-95% CI	eff.samp	pMCMC
(Intercept)	0.466385	0.233570	0.668693	1000.0	<0.001 ***
Reserve1	-0.093785	-0.365007	0.198831	921.3	0.550
Haul2	-0.249296	-0.509232	0.032707	1000.0	0.080 .
Haul3	-0.022553	-0.277129	0.277527	1000.0	0.898
Haul4	-0.207796	-0.469594	0.068030	1000.0	0.154
Haul5	-0.202905	-0.494439	0.060880	900.0	0.152
Haul6	-0.183580	-0.444051	0.091419	1000.0	0.196
Haul7	-0.255315	-0.532022 -	0.006161	1000.0	0.054 .
Haul8	-0.258903	-0.537076	0.021796	1000.0	0.076 .
Haul9	-0.307453	-0.570216	-0.008648	745.0	0.034 *
Haul10	-0.256212	-0.538086	-0.001027	911.6	0.054 .
Haul11	-0.277973	-0.566804	-0.004294	1000.0	0.058 .
Haul12	-0.268319	-0.520985	0.015278	1000.0	0.052 .
Haul13	-0.288087	-0.545656	-0.006317	1000.0	0.036 *
Haul14	-0.277553	-0.562426	0.005924	1000.0	0.066 .
Reserve1:Haul2	0.213581	-0.163629	0.604165	900.4	0.282
Reserve1:Haul3	0.168457	-0.224126	0.566261	1000.0	0.418
Reserve1:Haul4	0.020238	-0.360719	0.423651	842.7	0.926
Reserve1:Haul5	0.082630	-0.313355	0.480170	1000.0	0.704
Reserve1:Haul6	-0.009783	-0.420625	0.363147	1000.0	0.952
Reserve1:Haul7	0.071075	-0.294865	0.476844	1000.0	0.756
Reserve1:Haul8	0.080951	-0.345882	0.464960	1000.0	0.674
Reserve1:Haul9	0.122177	-0.294007	0.483843	1000.0	0.532
Reserve1:Haul10	0.071279	-0.336043	0.415399	1000.0	0.716
Reserve1:Haul11	0.057535	-0.317046	0.483580	842.1	0.760
Reserve1:Haul12	0.027979	-0.395676	0.403434	1000.0	0.890
Reserve1:Haul13	0.055587	-0.317476	0.495629	1129.7	0.796
Reserve1:Haul14	0.079727	-0.339673	0.474146	1000.0	0.694

Signif. codes: 0 ‘***’ 0.001 ‘**’ 0.01 ‘*’ 0.05 ‘.’ 0.1 ‘ ’ 1

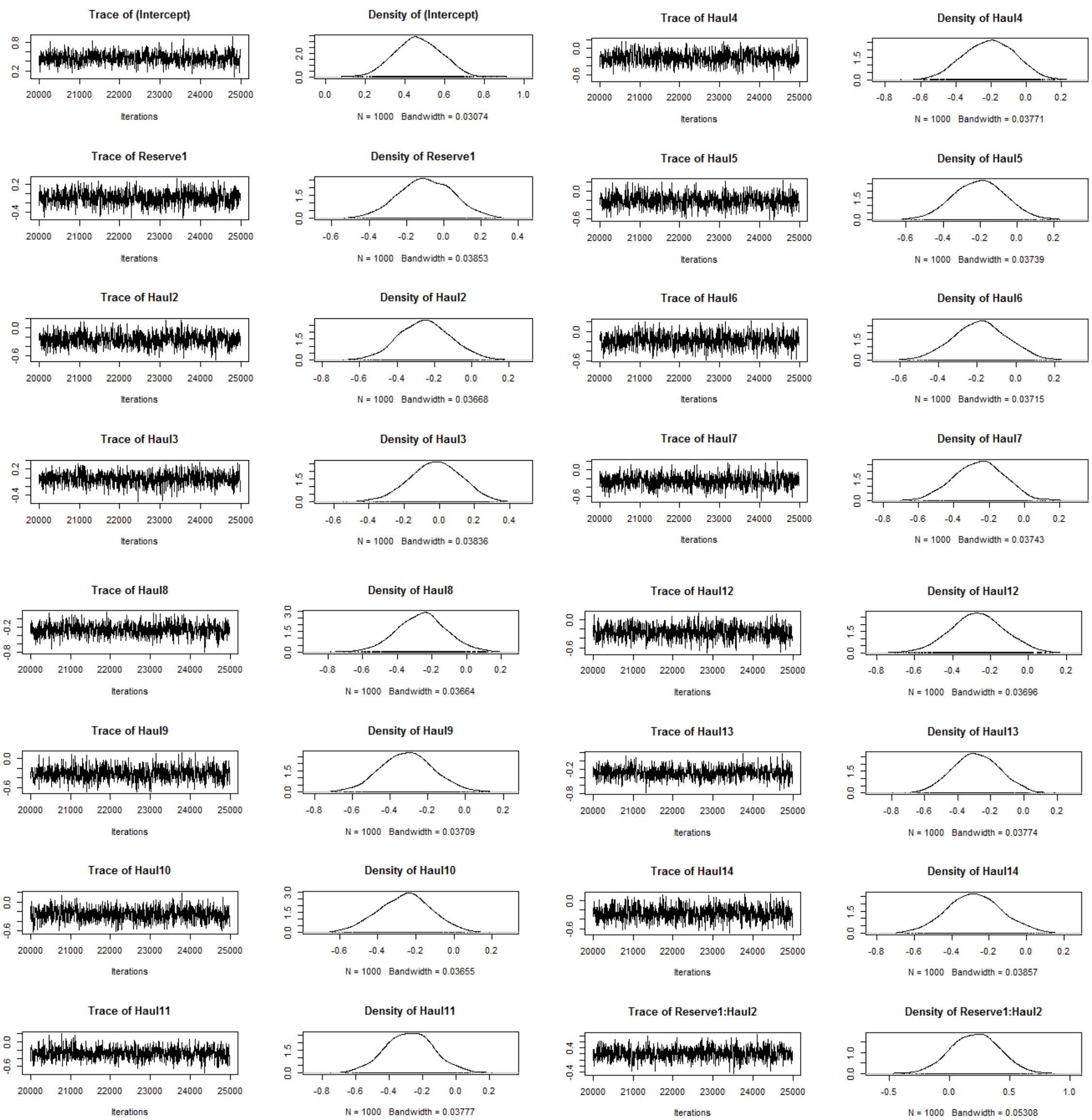
Trace of (Intercept)
Density of (Intercept)
N = 1000 Bandwidth = 0.03074
Trace of Haul4
Density of Haul4
N = 1000 Bandwidth = 0.03771
Trace of Reserve1
Density of Reserve1
N = 1000 Bandwidth = 0.03853
Trace of Haul5
Density of Haul5
N = 1000 Bandwidth = 0.03739
Trace of Haul2
Density of Haul2
N = 1000 Bandwidth = 0.03668
Trace of Haul6
Density of Haul6
N = 1000 Bandwidth = 0.03715
Trace of Haul3
Density of Haul3
N = 1000 Bandwidth = 0.03836
Trace of Haul7
Density of Haul7
N = 1000 Bandwidth = 0.03743
Trace of Haul8
Density of Haul8
N = 1000 Bandwidth = 0.03664
Trace of Haul12
Density of Haul12
N = 1000 Bandwidth = 0.03696
Trace of Haul9
Density of Haul9
N = 1000 Bandwidth = 0.03709
Trace of Haul13
Density of Haul13
N = 1000 Bandwidth = 0.03774
Trace of Haul10
Density of Haul10
N = 1000 Bandwidth = 0.03655
Trace of Haul14
Density of Haul14
N = 1000 Bandwidth = 0.03857
Trace of Haul11
Density of Haul11
N = 1000 Bandwidth = 0.03777
Trace of Reserve1:Haul2
Density of Reserve1:Haul2
N = 1000 Bandwidth = 0.05308
Iterations

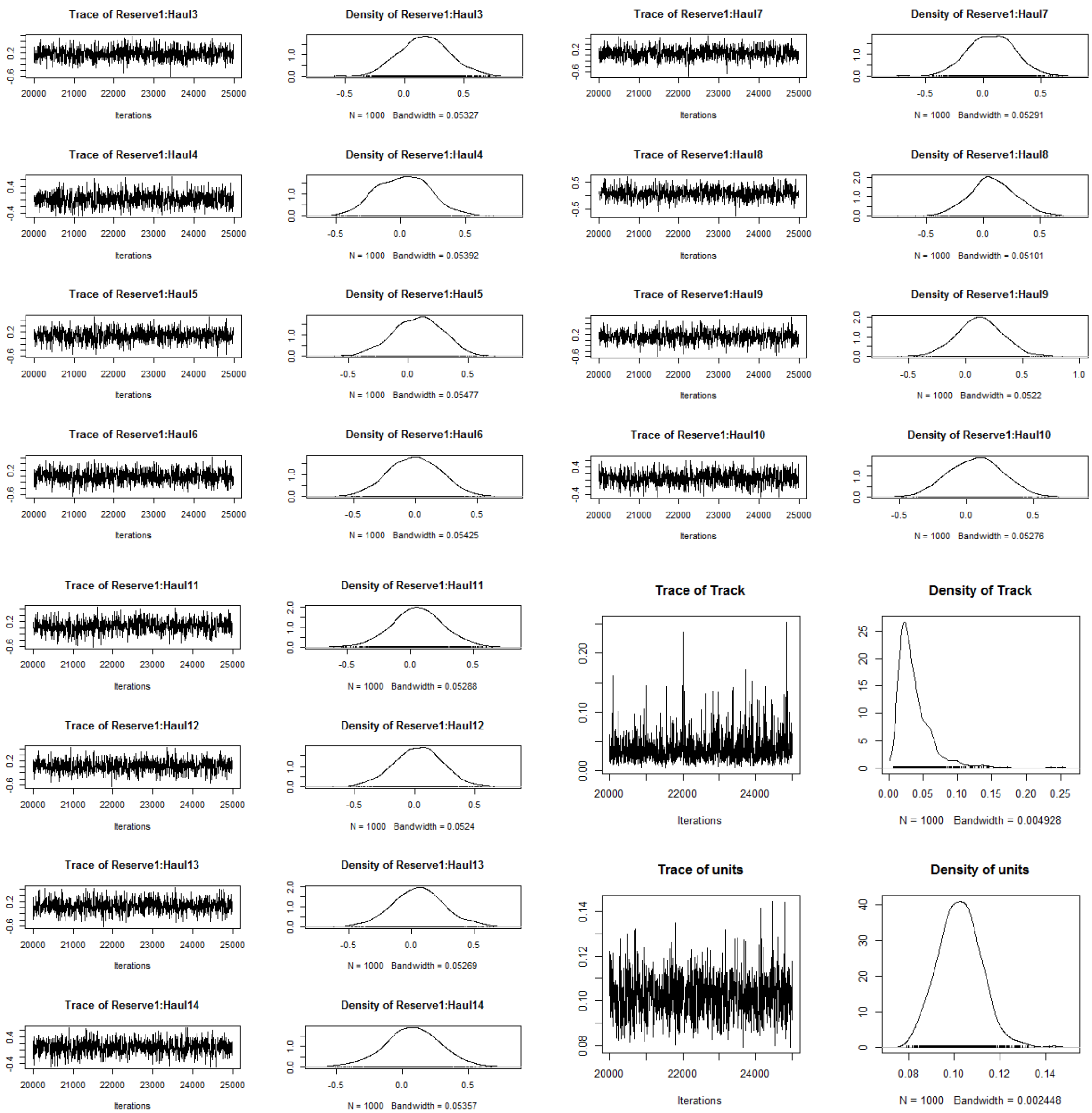

Trace of Reserve1:Haul3
Density of Reserve1:Haul3
N = 1000 Bandwidth = 0.05327
Trace of Reserve1:Haul7
Density of Reserve1:Haul7
N = 1000 Bandwidth = 0.05291
Trace of Reserve1:Haul4
Density of Reserve1:Haul4
N = 1000 Bandwidth = 0.05392
Trace of Reserve1:Haul8
Density of Reserve1:Haul8
N = 1000 Bandwidth = 0.05101
Trace of Reserve1:Haul5
Density of Reserve1:Haul5
N = 1000 Bandwidth = 0.05477
Trace of Reserve1:Haul9
Density of Reserve1:Haul9
N = 1000 Bandwidth = 0.0522
Trace of Reserve1:Haul6
Density of Reserve1:Haul6
N = 1000 Bandwidth = 0.05425
Trace of Reserve1:Haul10
Density of Reserve1:Haul10
N = 1000 Bandwidth = 0.05276
Trace of Reserve1:Haul11
Density of Reserve1:Haul11
N = 1000 Bandwidth = 0.05288
Trace of Track
Density of Track
N = 1000 Bandwidth = 0.004928
Trace of Reserve1:Haul12
Density of Reserve1:Haul12
N = 1000 Bandwidth = 0.0524
Trace of Reserve1:Haul13
Density of Reserve1:Haul13
N = 1000 Bandwidth = 0.05269
Trace of units
Density of units
N = 1000 Bandwidth = 0.002448
Trace of Reserve1:Haul14
Density of Reserve1:Haul14
N = 1000 Bandwidth = 0.05357
Iterations

Table A.2. Trace plots for parameters estimated by the Bayesian GLMM that include the proportion of downed sea whips within impact and control areas.

#model notation <- MCMCglmm(cbind(success,failure)~Reserve + Haul + Reserve:Haul, random =~Track,data=temp.dat,family="multinomial2", verbose=F, nitt=100000, burnin=75000, thin=25,pr=TRUE)

Summary of MCMCglmm

Iterations = 75001:99976 Thinning interval = 25 Sample size = 1000

DIC: 16182.72

G-structure: ~Track

	post.mean	l-95% CI	u-95% CI	eff.samp
Track	0.2635	0.05015	0.5864	1942

R-structure: ~units

	post.mean	l-95% CI	u-95% CI	eff.samp
units	0.2407	0.1674	0.3214	887.2

Location effects: cbind(success, failure) ~ Reserve + Haul + Reserve:Haul

	post.mean	l-95% CI	u-95% CI	eff.samp	pMCMC
(Intercept)	-1.66391	-2.20547	-1.15688	904.1	<0.001 ***
Reserve1	-0.79121	-1.31318	-0.17201	1000.0	0.012 *
Haul2	0.57289	-0.02467	1.13142	1000.0	0.052 .
Haul3	-0.53968	-1.13978	0.07498	603.0	0.084 .
Haul4	0.13337	-0.42882	0.77979	1000.0	0.650
Haul5	-0.38622	-1.02178	0.16877	1000.0	0.204
Haul6	0.64708	0.13926	1.20944	881.9	0.018 *
Haul7	-0.25838	-0.79570	0.40649	1000.0	0.388
Haul8	0.05642	-0.48714	0.72049	586.7	0.862
Haul9	-0.40585	-1.05234	0.33823	1000.0	0.270
Haul10	0.31883	-0.24442	0.88801	1000.0	0.298
Haul11	-0.24654	-0.84870	0.37064	1000.0	0.444
Haul12	-0.12646	-0.71158	0.46879	889.1	0.700
Haul13	0.04894	-0.55956	0.57157	536.3	0.892
Haul14	0.28117	-0.35577	0.82815	1000.0	0.362
Reserve1:Haul2	-0.47027	-1.22769	0.41518	1000.0	0.252
Reserve1:Haul3	0.26426	-0.48970	1.16540	1000.0	0.528
Reserve1:Haul4	-0.09664	-0.79507	0.73403	897.8	0.804
Reserve1:Haul5	0.39672	-0.44785	1.14996	1000.0	0.358
Reserve1:Haul6	-0.64567	-1.43062	0.15842	1000.0	0.114
Reserve1:Haul7	0.26350	-0.48915	1.12648	1000.0	0.476
Reserve1:Haul8	0.45430	-0.30149	1.36548	1000.0	0.282
Reserve1:Haul9	0.49740	-0.45756	1.33044	1000.0	0.250
Reserve1:Haul10	-0.20396	-1.01427	0.54915	1000.0	0.646
Reserve1:Haul11	0.54861	-0.26005	1.35295	737.3	0.170
Reserve1:Haul12	0.26559	-0.44796	1.17020	1000.0	0.528
Reserve1:Haul13	-0.11035	-0.90410	0.74192	1000.0	0.808
Reserve1:Haul14	-0.78531	-1.62169	0.19807	910.1	0.092 .

---Signif. codes: 0 ‘***’ 0.001 ‘**’ 0.01 ‘*’ 0.05 ‘.’ 0.1 ‘ ’ 1

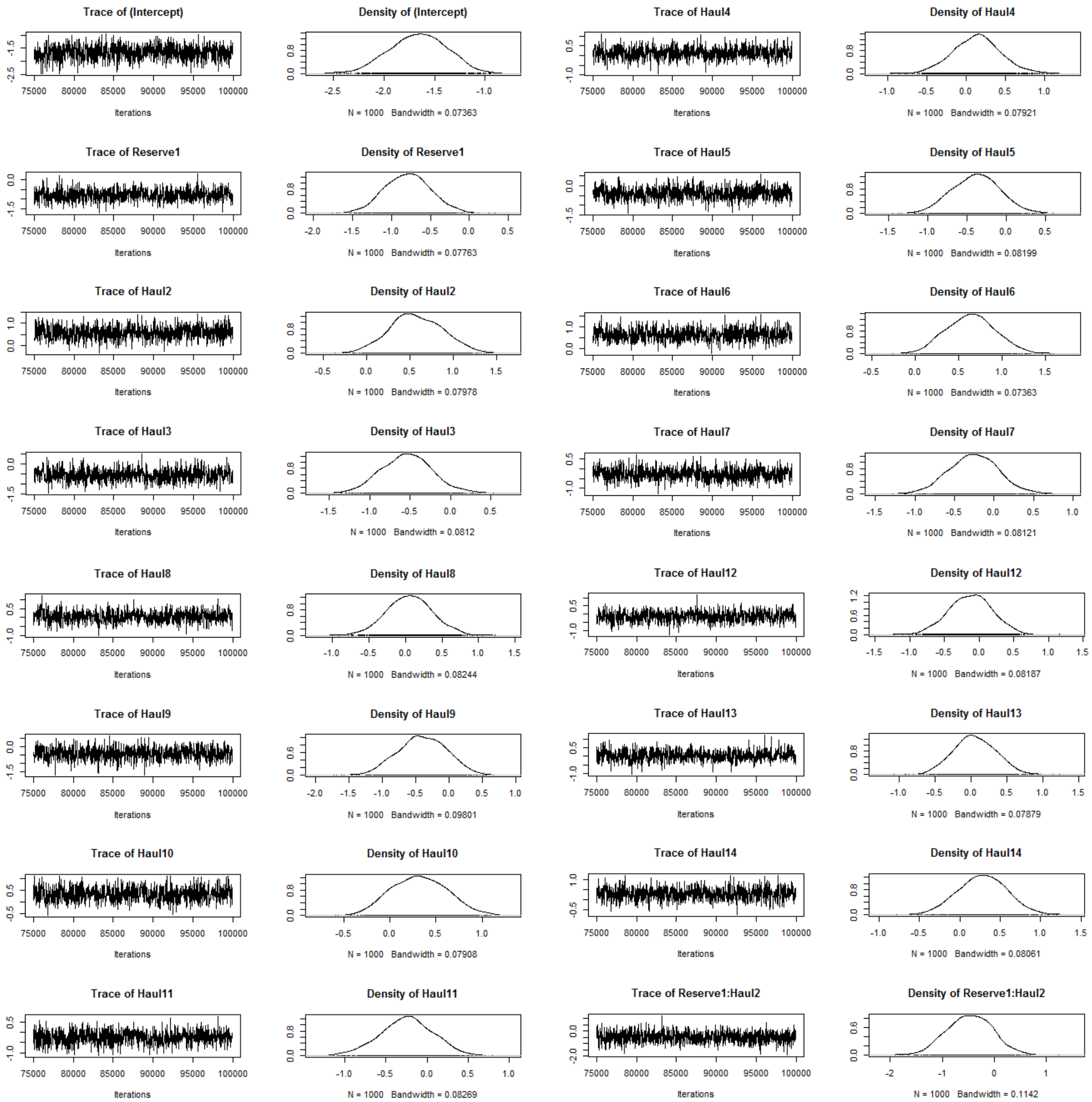
Trace of (Intercept)
Iterations
Density of (Intercept)
N = 1000 Bandwidth = 0.07363
Trace of Haul4
Iterations
Density of Haul4
N = 1000 Bandwidth = 0.07921
Trace of Reserve1
Iterations
Density of Reserve1
N = 1000 Bandwidth = 0.07763
Trace of Haul5
Iterations
Density of Haul5
N = 1000 Bandwidth = 0.08199
Trace of Haul2
Iterations
Density of Haul2
N = 1000 Bandwidth = 0.07978
Trace of Haul6
Iterations
Density of Haul6
N = 1000 Bandwidth = 0.07363
Trace of Haul3
Iterations
Density of Haul3
N = 1000 Bandwidth = 0.0812
Trace of Haul7
Iterations
Density of Haul7
N = 1000 Bandwidth = 0.08121
Trace of Haul8
Iterations
Density of Haul8
N = 1000 Bandwidth = 0.08244
Trace of Haul12
Iterations
Density of Haul12
N = 1000 Bandwidth = 0.08187
Trace of Haul9
Iterations
Density of Haul9
N = 1000 Bandwidth = 0.09801
Trace of Haul13
Iterations
Density of Haul13
N = 1000 Bandwidth = 0.07879
Trace of Haul10
Iterations
Density of Haul10
N = 1000 Bandwidth = 0.07908
Trace of Haul14
Iterations
Density of Haul14
N = 1000 Bandwidth = 0.08061
Trace of Haul11
Iterations
Density of Haul11
N = 1000 Bandwidth = 0.08269
Trace of Reserve1:Haul2
Iterations
Density of Reserve1:Haul2
N = 1000 Bandwidth = 0.1142

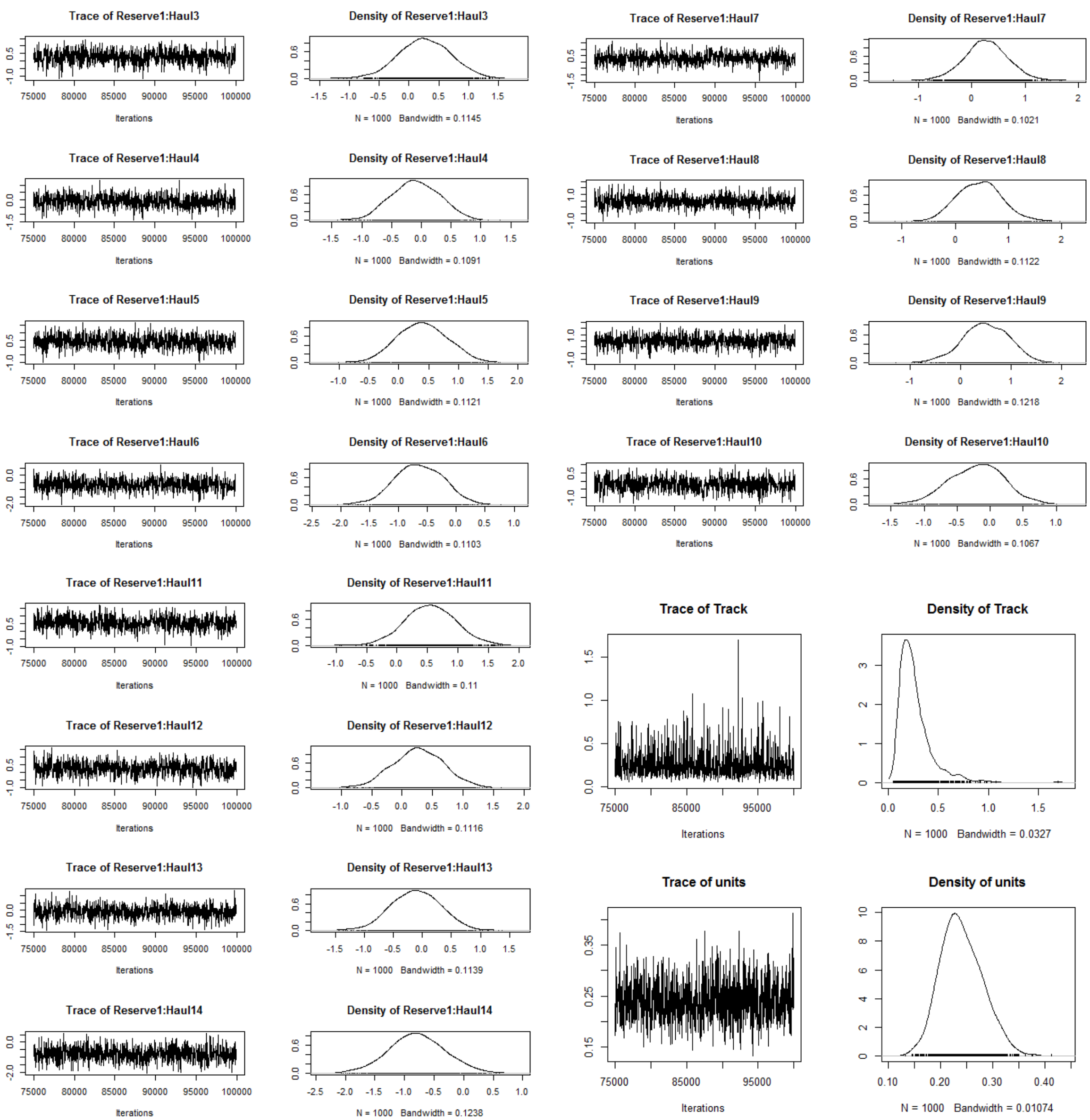
Trace of Reserve1:Haul3
Iterations
Density of Reserve1:Haul3
N = 1000 Bandwidth = 0.1145
Trace of Reserve1:Haul7
Iterations
Density of Reserve1:Haul7
N = 1000 Bandwidth = 0.1021
Trace of Reserve1:Haul4
Iterations
Density of Reserve1:Haul4
N = 1000 Bandwidth = 0.1091
Trace of Reserve1:Haul8
Iterations
Density of Reserve1:Haul8
N = 1000 Bandwidth = 0.1122
Trace of Reserve1:Haul5
Iterations
Density of Reserve1:Haul5
N = 1000 Bandwidth = 0.1121
Trace of Reserve1:Haul9
Iterations
Density of Reserve1:Haul9
N = 1000 Bandwidth = 0.1218
Trace of Reserve1:Haul6
Iterations
Density of Reserve1:Haul6
N = 1000 Bandwidth = 0.1103
Trace of Reserve1:Haul10
Iterations
Density of Reserve1:Haul10
N = 1000 Bandwidth = 0.1067
Trace of Reserve1:Haul11
Iterations
Density of Reserve1:Haul11
N = 1000 Bandwidth = 0.11
Trace of Track
Iterations
Density of Track
N = 1000 Bandwidth = 0.0327
Trace of Reserve1:Haul12
Iterations
Density of Reserve1:Haul12
N = 1000 Bandwidth = 0.1116
Trace of Reserve1:Haul13
Iterations
Density of Reserve1:Haul13
N = 1000 Bandwidth = 0.1139
Trace of units
Iterations
Density of units
N = 1000 Bandwidth = 0.01074
Trace of Reserve1:Haul14
Iterations
Density of Reserve1:Haul14
N = 1000 Bandwidth = 0.1238

Table A.3. Trace plots for parameters estimated by the Bayesian GLMM that include the proportion of damaged sea whips within impact and control.

#model notation <- MCMCglmm(cbind(success,failure)~Reserve + Haul + Reserve:Haul, random = ~Track,data=temp.dat,family="multinomial2", verbose=F, nitt=100000, burnin=75000, thin=25,pr=TRUE)

Summary of MCMCglmm

Iterations = 75001:99976 Thinning interval = 25 Sample size = 1000

DIC: 3015.713

G-structure: ~Track

	post.mean	l-95% C	l u-95% CI	eff.samp
Track	3.081	0.3414	6.824	883

R-structure: ~units

	post.mean	l-95% CI	u-95% CI	eff.samp
units	3.286	2.056	4.878	578.3

Location effects: cbind(success, failure) ~ Reserve + Haul + Reserve:Haul

	post.mean	l-95% CI	u-95% CI	eff.samp	pMCMC
(Intercept)	-5.12998	-7.26200	-3.39960	1000.0	<0.001 ***
Reserve1	-1.03375	-3.07187	1.28798	1504.0	0.322
Haul2	0.92703	-1.09346	3.07360	1000.0	0.358
Haul3	-1.25304	-3.72677	0.86693	1000.0	0.262
Haul4	-1.33965	-3.71037	1.12840	1000.0	0.264
Haul5	-0.09588	-2.28532	2.15872	1000.0	0.932
Haul6	1.12626	-0.90667	3.09328	1000.0	0.280
Haul7	0.21431	-1.80252	2.45638	1337.3	0.836
Haul8	-1.34072	-3.89622	1.46098	905.5	0.332
Haul9	-0.24575	-2.89274	1.95067	863.8	0.866
Haul10	0.41573	-1.65123	2.48192	1159.3	0.688
Haul11	-0.57327	-2.72090	1.96192	1055.2	0.652
Haul12	0.33195	-1.93921	2.26881	1000.0	0.784
Haul13	-0.04308	-2.31759	2.07475	1011.0	1.000
Haul14	0.22550	-1.90215	2.44078	1000.0	0.834
Reserve1:Haul2	-2.10967	-5.50568	1.28214	1000.0	0.214
Reserve1:Haul3	-2.67053	-6.74612	1.82130	545.8	0.210
Reserve1:Haul4	-0.47852	-3.60528	3.62276	1130.0	0.796
Reserve1:Haul5	-1.22311	-4.37878	2.40148	1476.3	0.484
Reserve1:Haul6	-2.41611	-5.40022	1.16089	912.8	0.152
Reserve1:Haul7	-1.61837	-5.12927	1.42311	1085.0	0.354
Reserve1:Haul8	-0.72538	-5.41333	2.73330	952.1	0.758
Reserve1:Haul9	0.16824	-3.39253	3.35487	1000.0	0.888
Reserve1:Haul10	-0.57916	-3.81075	1.94448	1111.1	0.750
Reserve1:Haul11	0.23834	-2.90622	3.44974	1159.8	0.904
Reserve1:Haul12	-0.04882	-2.86201	3.13336	884.6	0.970
Reserve1:Haul13	-1.10872	-4.65671	2.19211	1000.0	0.542
Reserve1:Haul14	-1.45961	-5.14880	2.13455	880.8	0.424

Signif. codes: 0 ‘***’ 0.001 ‘**’ 0.01 ‘*’ 0.05 ‘.’ 0.1 ‘ ’ 1

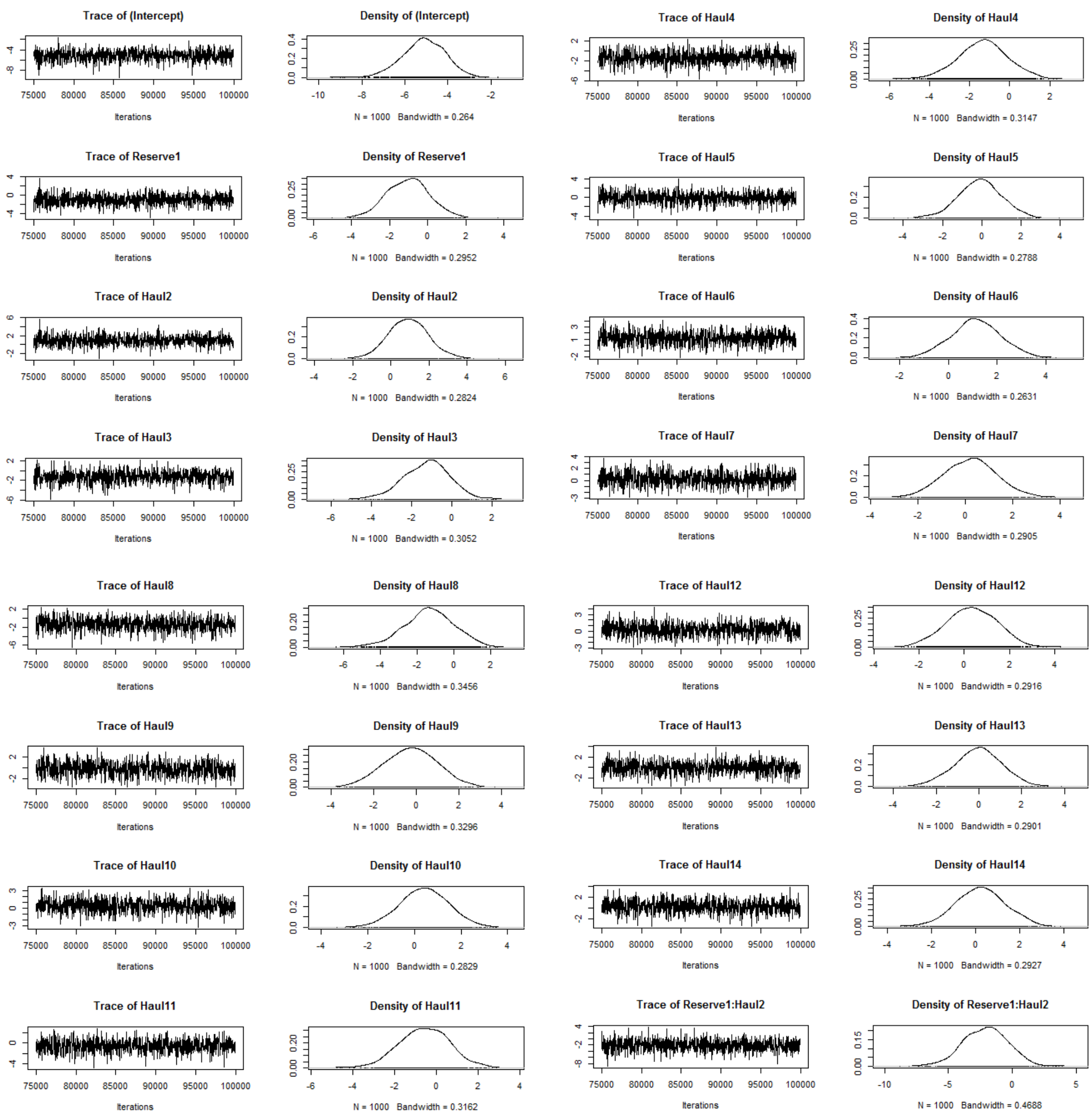
Trace of (Intercept)
Density of (Intercept)
Trace of Haul4
Density of Haul4
Trace of Reserve1
Density of Reserve1
Trace of Haul5
Density of Haul5
Trace of Haul2
Density of Haul2
Trace of Haul6
Density of Haul6
Trace of Haul3
Density of Haul3
Trace of Haul7
Density of Haul7
Trace of Haul8
Density of Haul8
Trace of Haul12
Density of Haul12
Trace of Haul9
Density of Haul9
Trace of Haul13
Density of Haul13
Trace of Haul10
Density of Haul10
Trace of Haul14
Density of Haul14
Trace of Haul11
Density of Haul11
Trace of Reserve1:Haul2
Density of Reserve1:Haul2

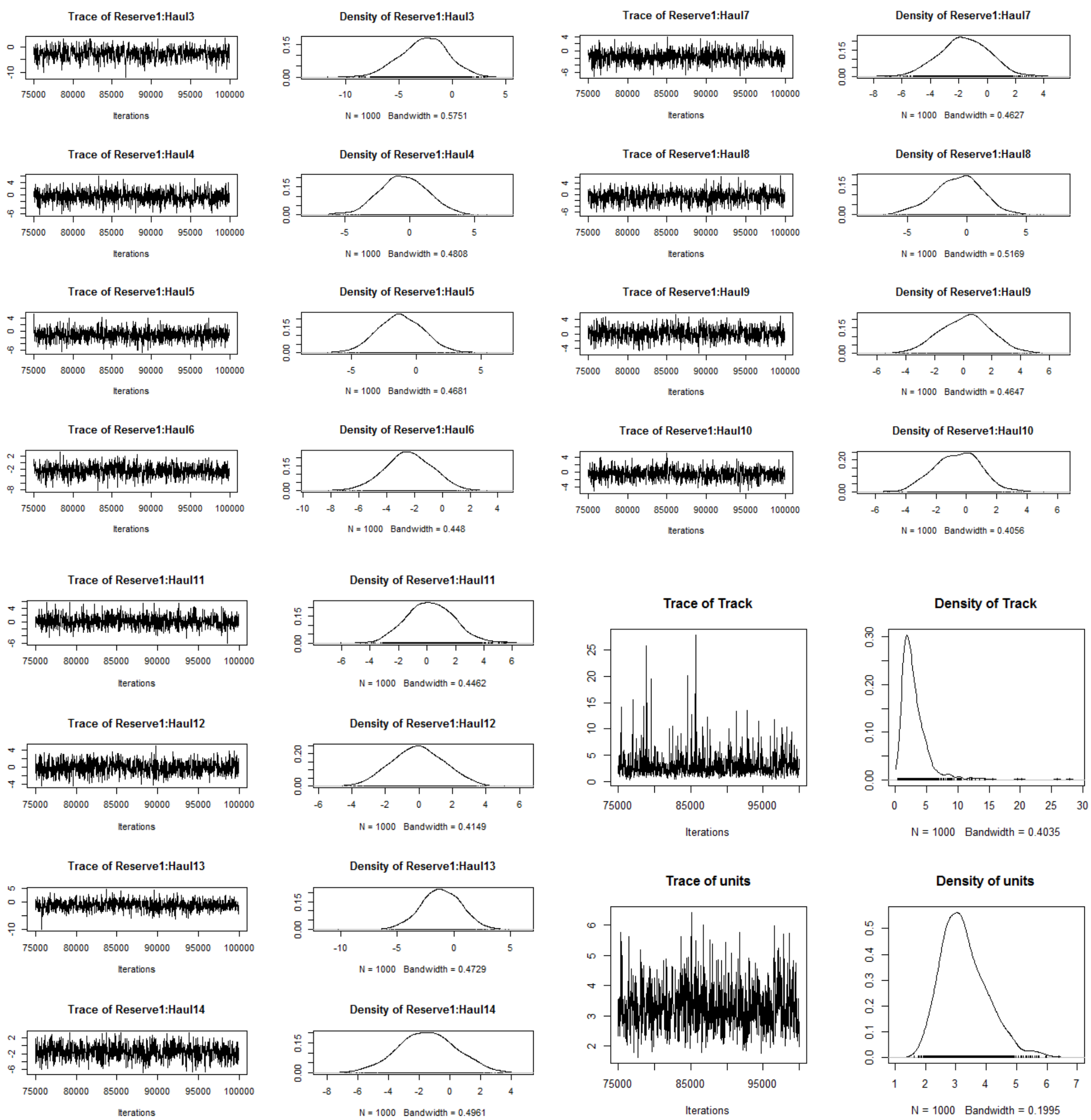

Trace of Reserve1:Haul3
Density of Reserve1:Haul3
N = 1000 Bandwidth = 0.5751
Trace of Reserve1:Haul7
Density of Reserve1:Haul7
N = 1000 Bandwidth = 0.4627
Trace of Reserve1:Haul4
Density of Reserve1:Haul4
N = 1000 Bandwidth = 0.4808
Trace of Reserve1:Haul8
Density of Reserve1:Haul8
N = 1000 Bandwidth = 0.5169
Trace of Reserve1:Haul5
Density of Reserve1:Haul5
N = 1000 Bandwidth = 0.4681
Trace of Reserve1:Haul9
Density of Reserve1:Haul9
N = 1000 Bandwidth = 0.4647
Trace of Reserve1:Haul6
Density of Reserve1:Haul6
N = 1000 Bandwidth = 0.448
Trace of Reserve1:Haul10
Density of Reserve1:Haul10
N = 1000 Bandwidth = 0.4056
Trace of Reserve1:Haul11
Density of Reserve1:Haul11
N = 1000 Bandwidth = 0.4462
Trace of Track
Density of Track
N = 1000 Bandwidth = 0.4035
Trace of Reserve1:Haul12
Density of Reserve1:Haul12
N = 1000 Bandwidth = 0.4149
Trace of Reserve1:Haul13
Density of Reserve1:Haul13
N = 1000 Bandwidth = 0.4729
Trace of units
Density of units
N = 1000 Bandwidth = 0.1995
Trace of Reserve1:Haul14
Density of Reserve1:Haul14
N = 1000 Bandwidth = 0.4961
Iterations

Table A.4. Frequency of seafloor clearance measurements by material in all the mid-span locations on the footrope.
Note: noise from the sensors is seen in the high frequency of measurements less than 1 in. These data were not included in the results of this thesis, but lead to future work.

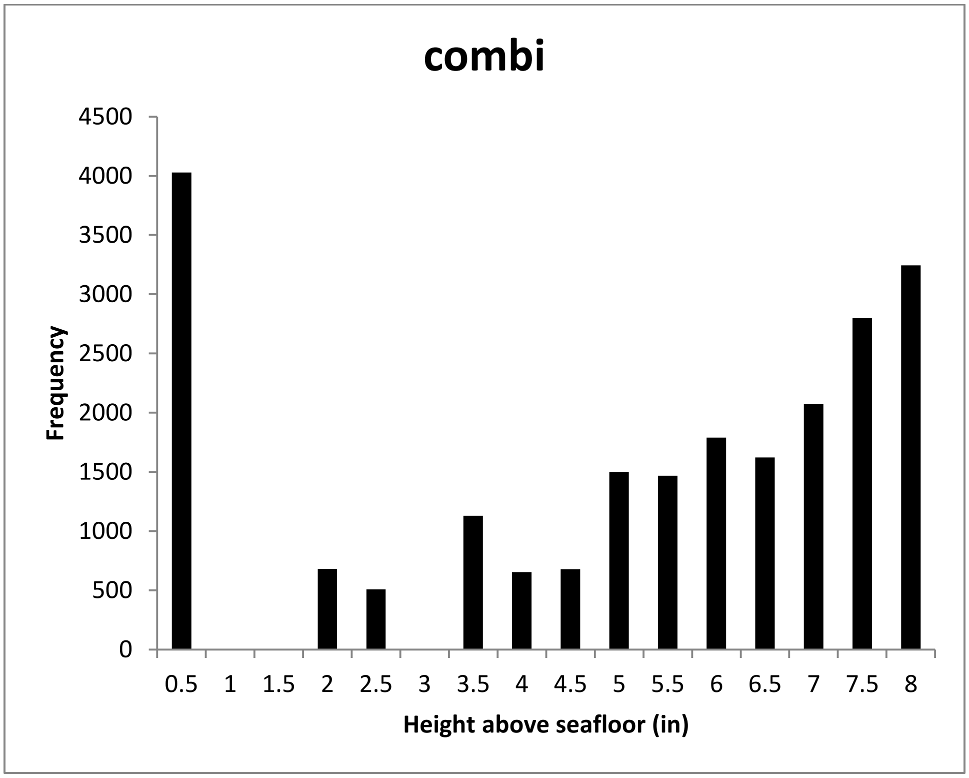

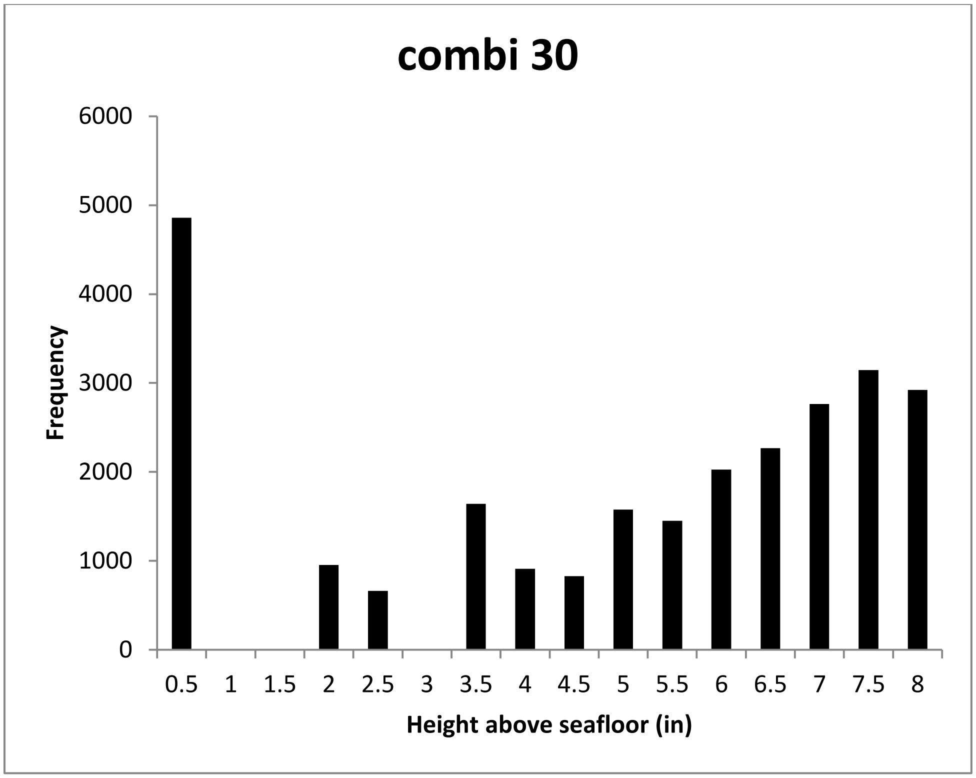
combi 30
6000
5000
4000
3000
2000
1000
0
Frequency
0.5 1 1.5 2 2.5 3 3.5 4 4.5 5 5.5 6 6.5 7 7.5 8
Height above seafloor (in)

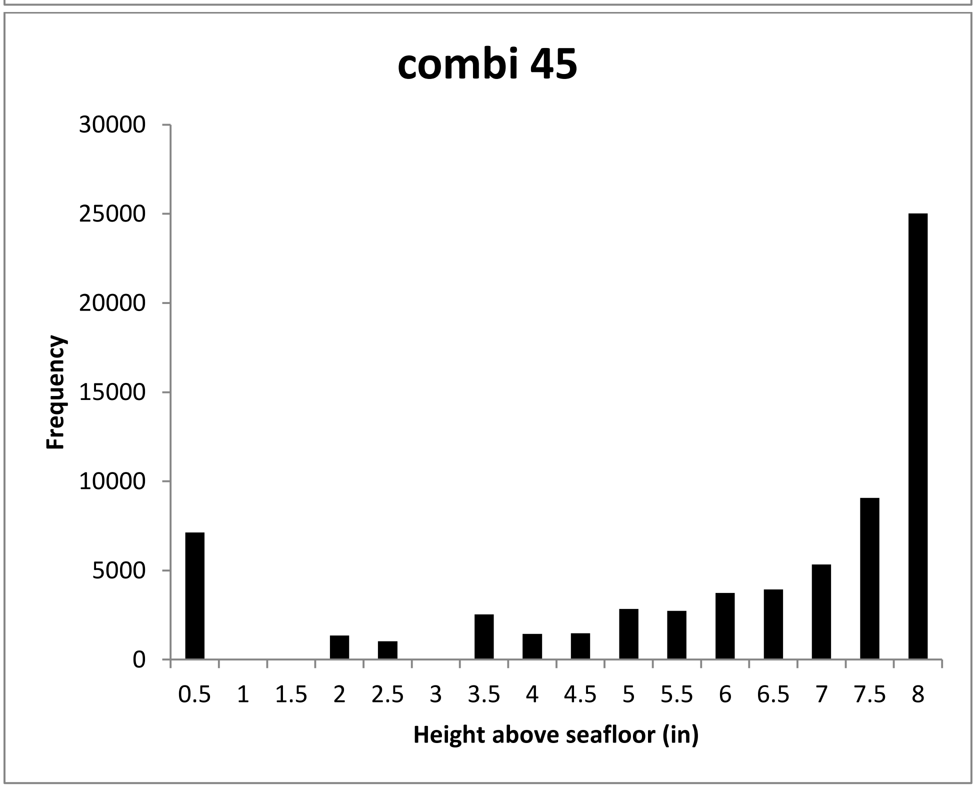
combi 45
30000
25000
20000
15000
10000
5000
0
Frequency
0.5 1 1.5 2 2.5 3 3.5 4 4.5 5 5.5 6 6.5 7 7.5 8
Height above seafloor (in)

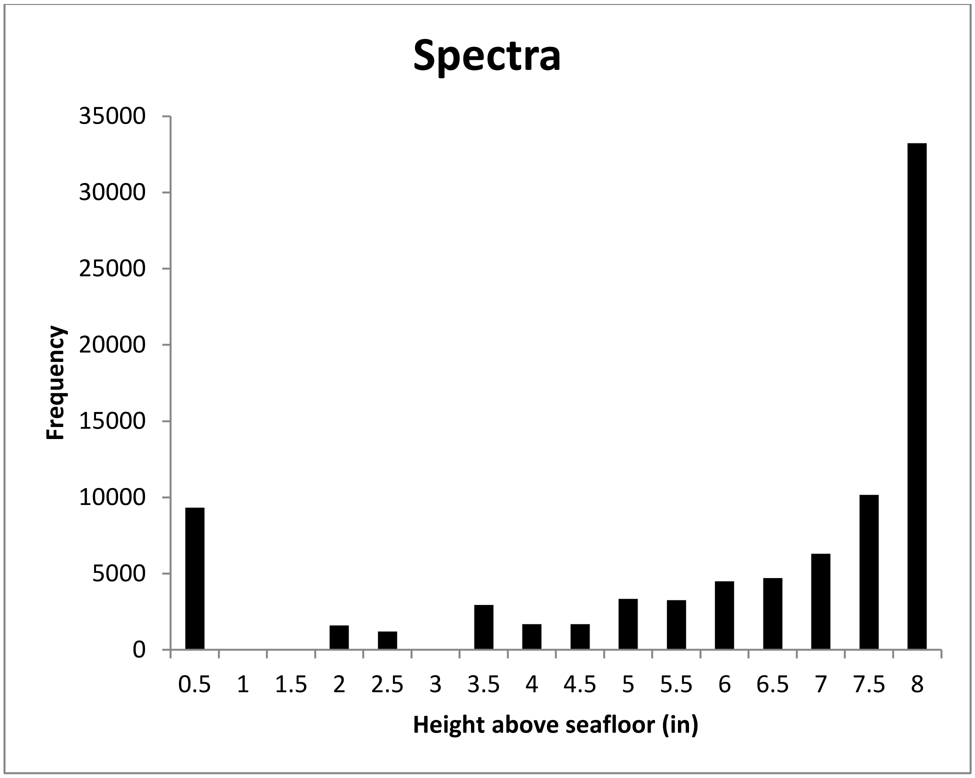
Spectra
Frequency
35000
30000
25000
20000
15000
10000
5000
0
0.5 1 1.5 2 2.5 3 3.5 4 4.5 5 5.5 6 6.5 7 7.5 8
Height above seafloor (in)

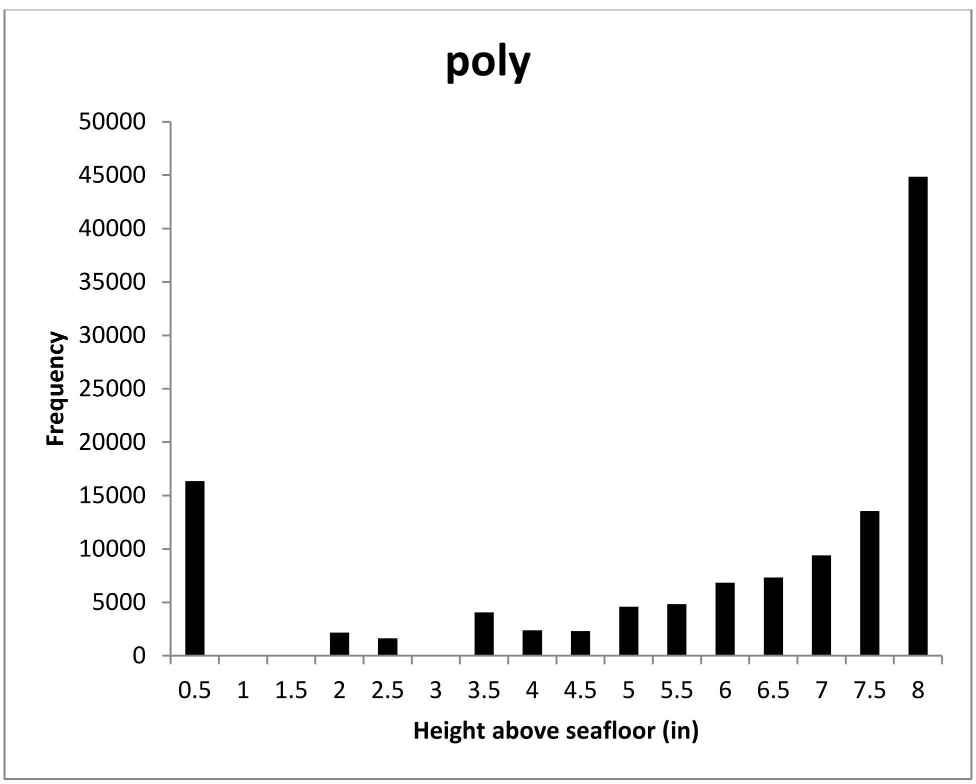
poly
Frequency
50000
45000
40000
35000
30000
25000
20000
15000
10000
5000
0
0.5 1 1.5 2 2.5 3 3.5 4 4.5 5 5.5 6 6.5 7 7.5 8
Height above seafloor (in)